Cosmic Structure Formation: far-UV/Soft X-ray spectroscopy

Qingde Daniel Wang (王青德)
University of Massachusetts
and NJU/PMO

Composition and structure formation of the universe

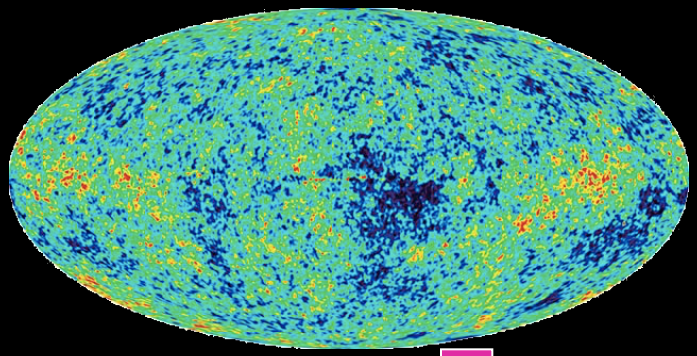

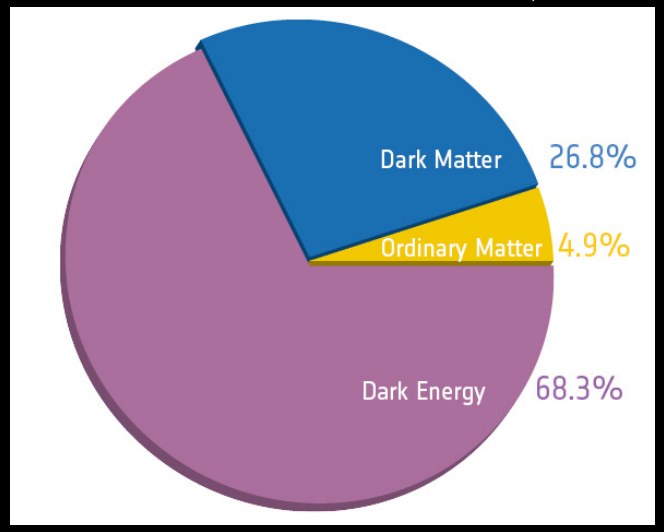

S. Bertone, A. Aguirre and J. Schaye (2013)

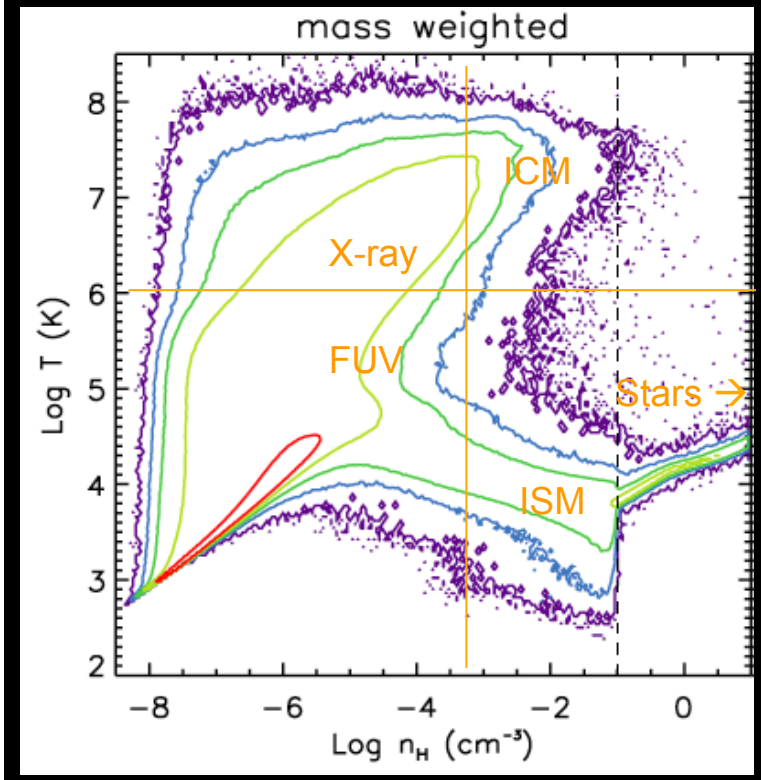

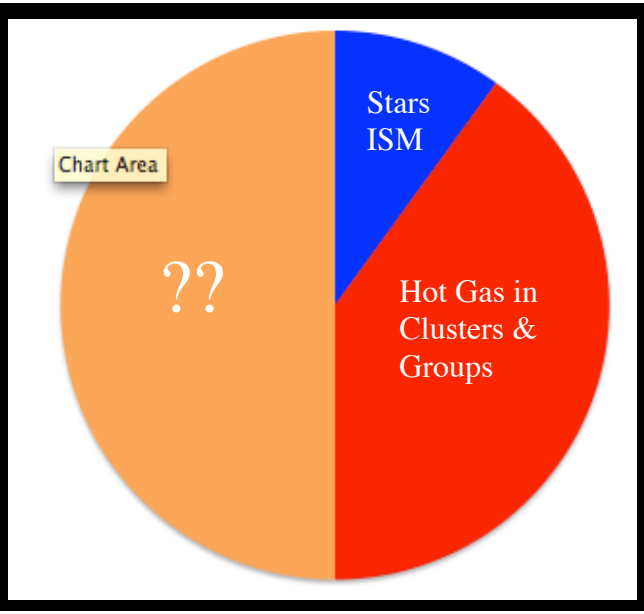

The CGM and IGM, as well as the ISM and ICM, are a feedback depository and a gas reservoir of galaxies and can be effectively traced by far-UV and soft X-ray, ideally via spectroscopy.

Quantifying the individual components and their interplay is fundamental to understanding the eco-systems of galaxies!

Previous and existing far-UV/soft X-ray spectroscopy capabilities

- Far-UV (almost exclusively for absorption line spectroscopy)
  - FUSE (905 - 1187 Å): the largest aperture (0.5′x0.5′) allowed for limited diffuse emission observations
  - HST/COS (1150-3200 Å): almost having no capability for diffuse emission
- X-ray: slit-less grating spectrometers, mostly for point-like emission
  - Chandra/LETG/HETG (0.2-8 keV)
  - XMM-Newtron/RGS (0.3-2 keV): large dispersion capability allows limited use for moderately extended, bright diffuse emission.

These limited capabilities have been explored, having yielded transformative results.

Lack of cool X-ray emitting gas

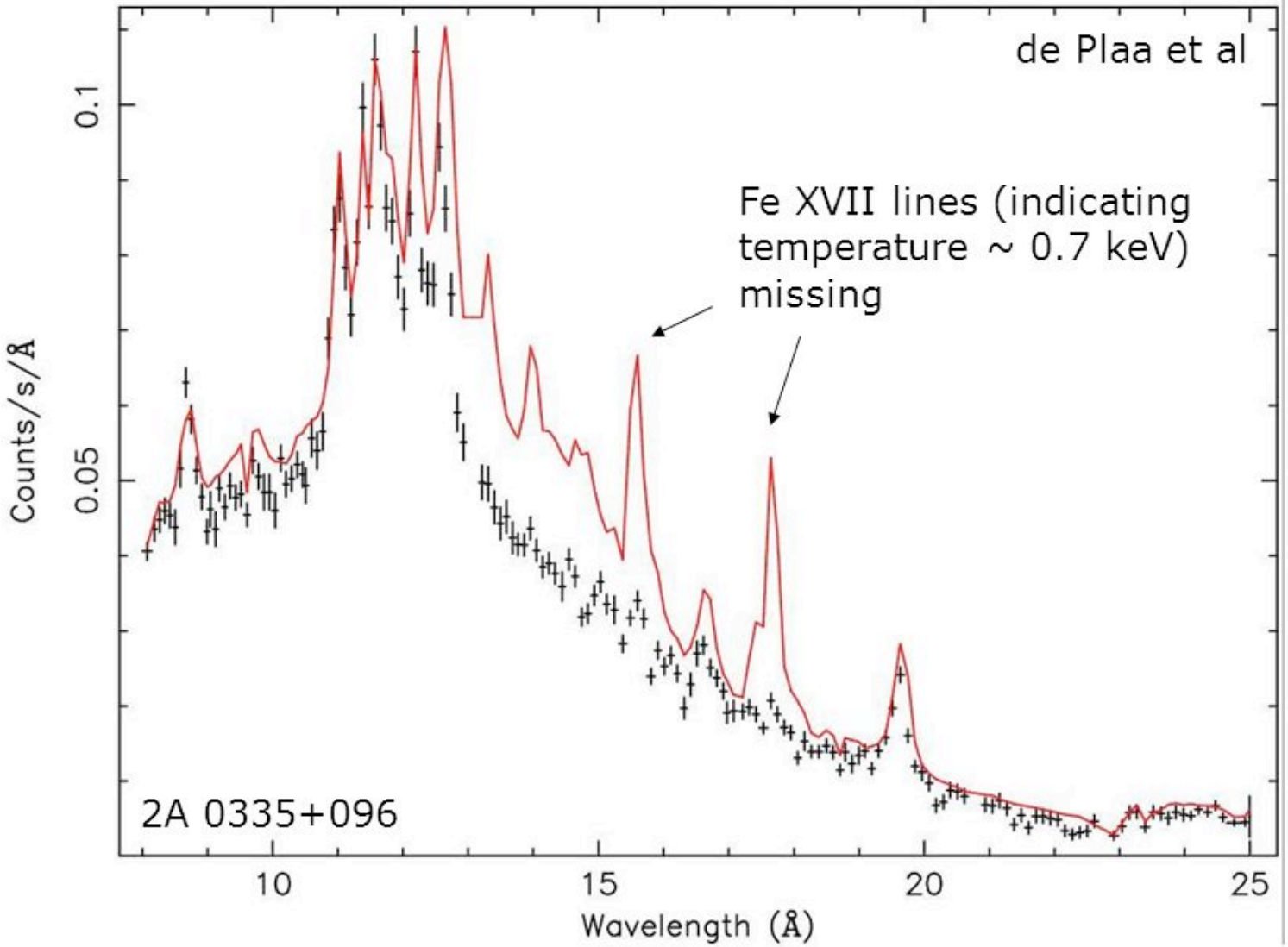

Slow cooling in the core of the galaxy cluster 2A 0335+096

Image courtesy of Jelle de Plaa, SRON, NL.

European Space Agency

Spectra imply less than 10% of cooling rates expected from luminosity profiles

Only significant gas down to 1/2 to 1/3 of outer temperature

AGN heating?

see also Peterson et al 01, 03, Kaastra et al 01, 03, Tamura et al 01,...

AGN feedback is apparently a solution to the cooling flow problem

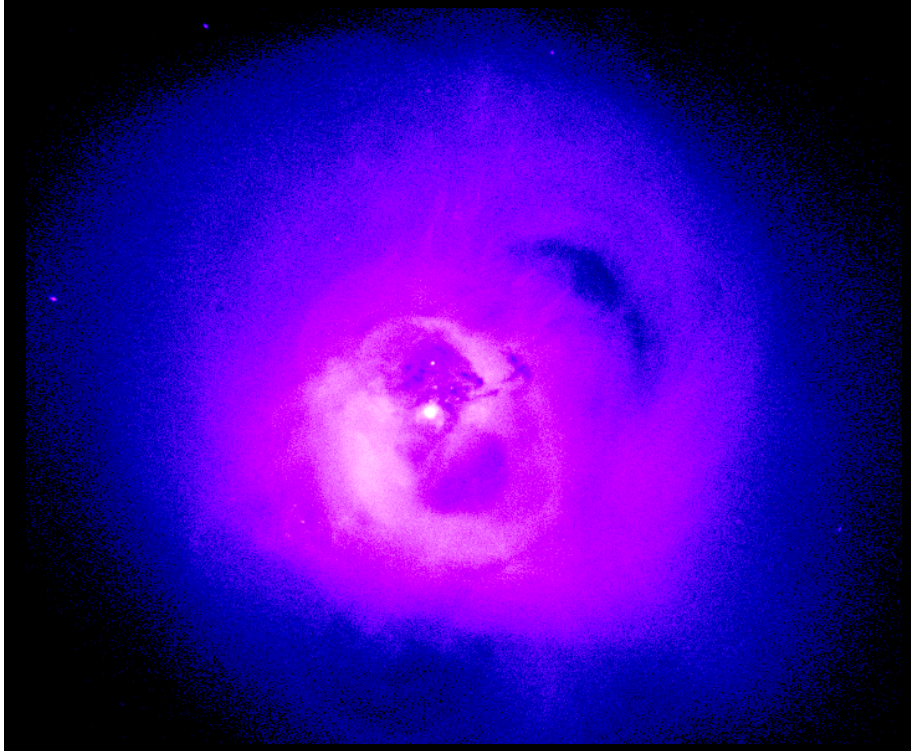

Hot Gas in the Perseus Cluster: 50 x 10^6 K

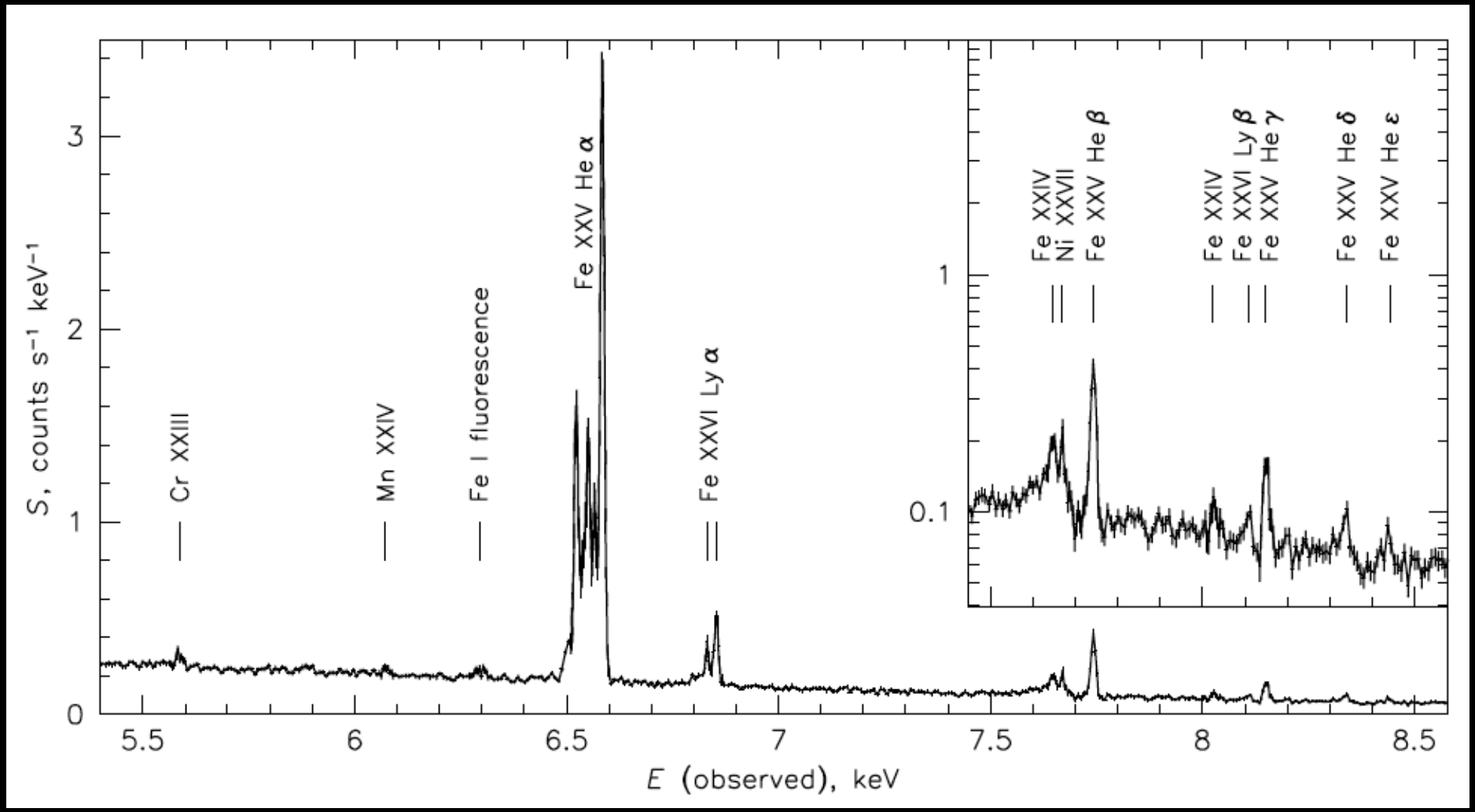

Hitomi Collaboration– Nature 264, 2016

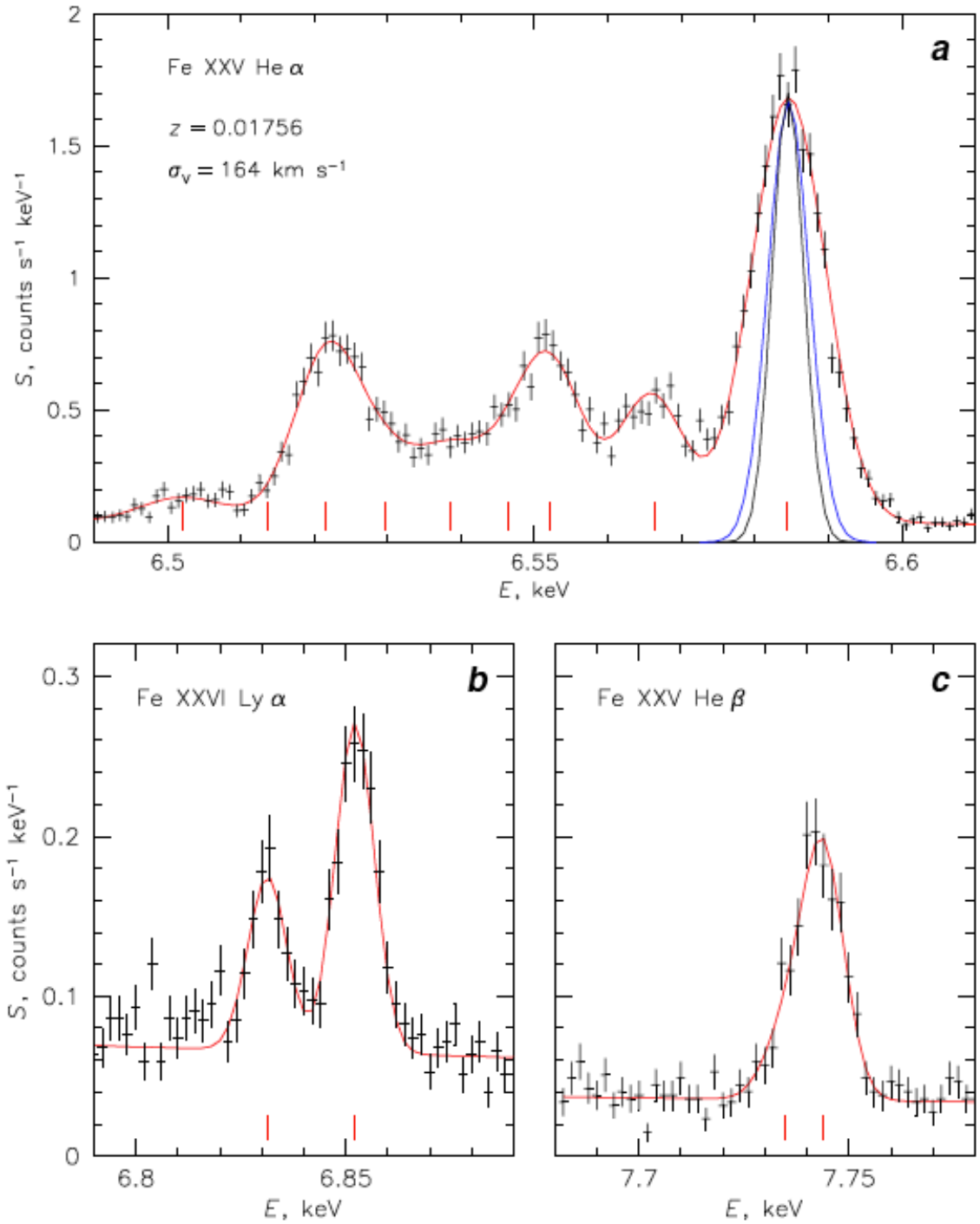

Resolving power ~1500
Allows accurate measurement of Doppler broadening of Fe lines (at an accuracy of ~10 km/s).
Can show that turbulence and shear are only about 4% of thermal pressure.

Hitomi Collaboration
Nature 264, 2016

XMM-Newton/RGS spectrum of massive elliptical galaxy NGC 4636

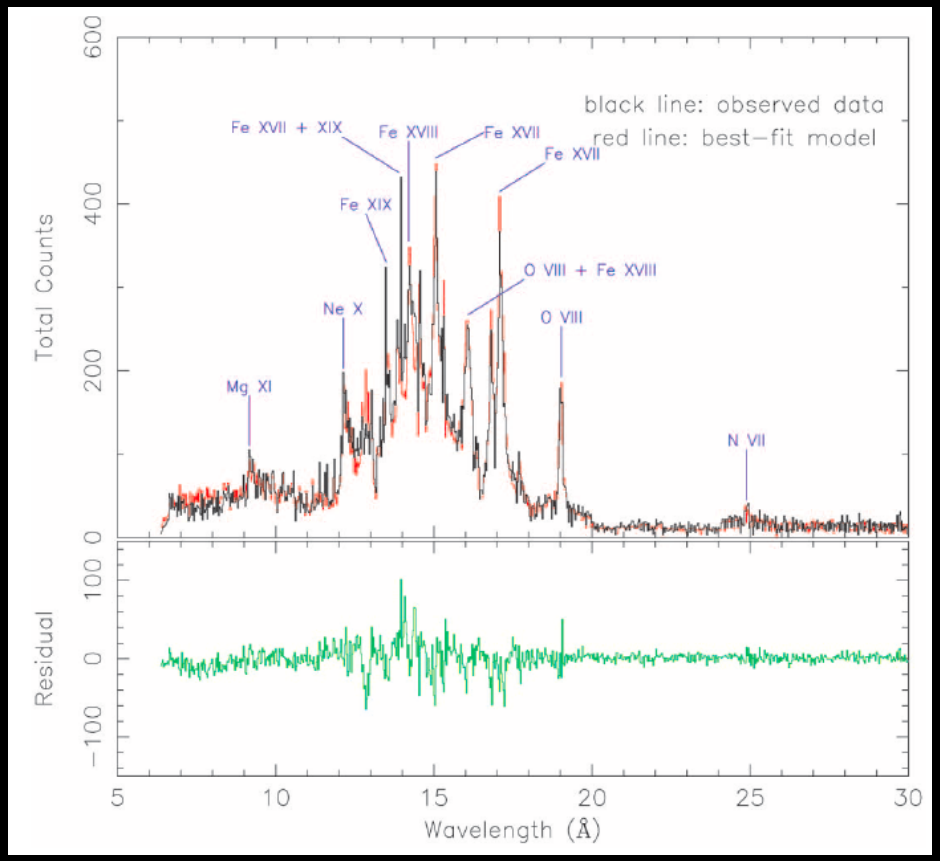

Xu et al. 02

- Strong resonance scattering effect on the 3d-2p 15.0 Å line, relative to the 3s-2p 16.0 and 17.1 Å lines of Fe XVII.
- Allow for estimate of the turbulent velocity dispersion of the ISM.
- Fe abundance is still lower than the theoretical expectation.

XMM-Newton RGS spectrum of the stellar bulge of M31

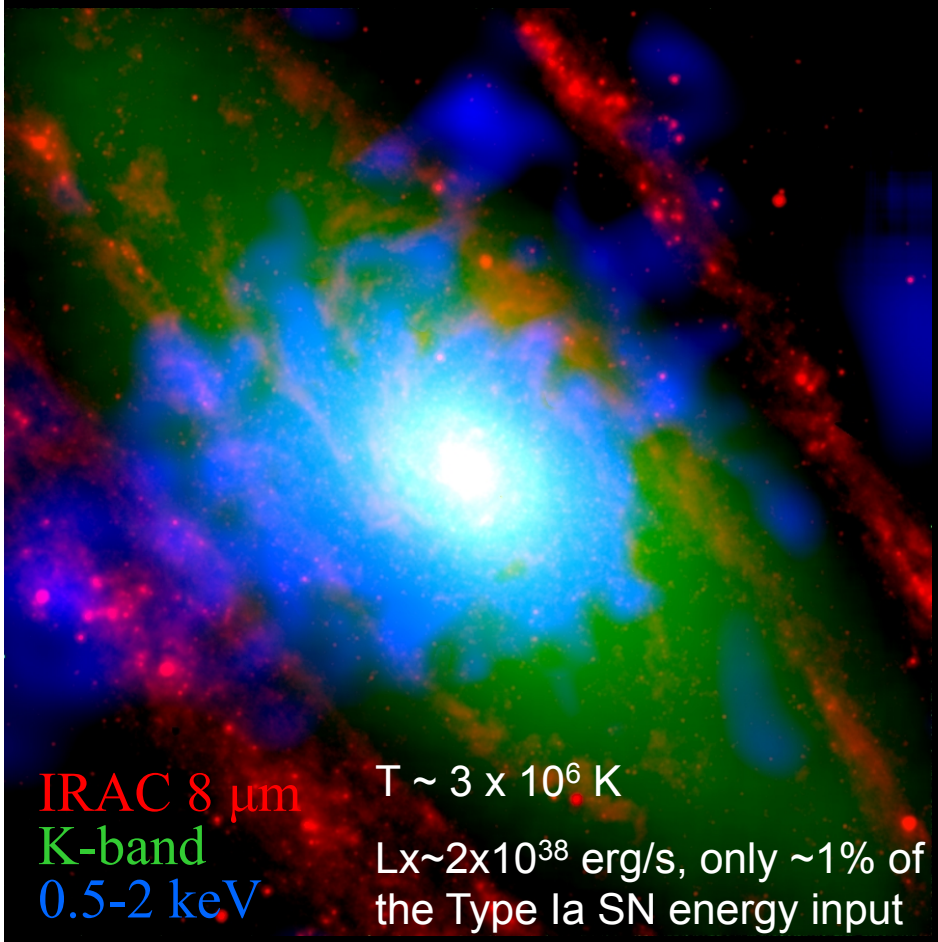

Li & Wang 2007

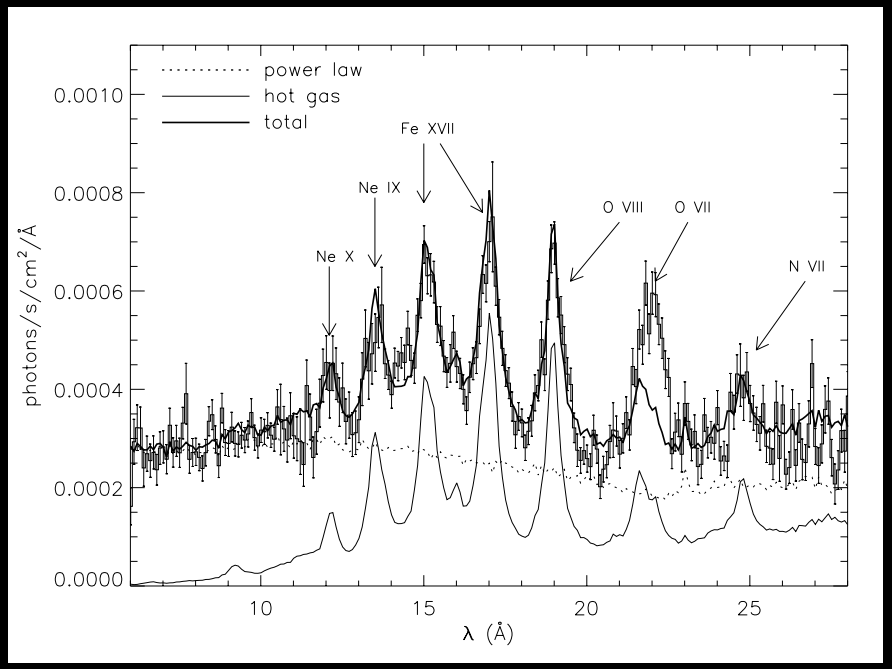

Strong deviation of the OVII Kα triplet from the thermal model: the forbidden line at 21.80 Å is much stronger than the resonance line at 21.60 Å.

Liu, Wang, Li, & Peterson 2010

Nature of the X-ray Emission: Line Spectroscopy

The resonance line is found to be weaker than the "forbidden"+"inter-recommbination" lines, which is not expected for thermal emission.

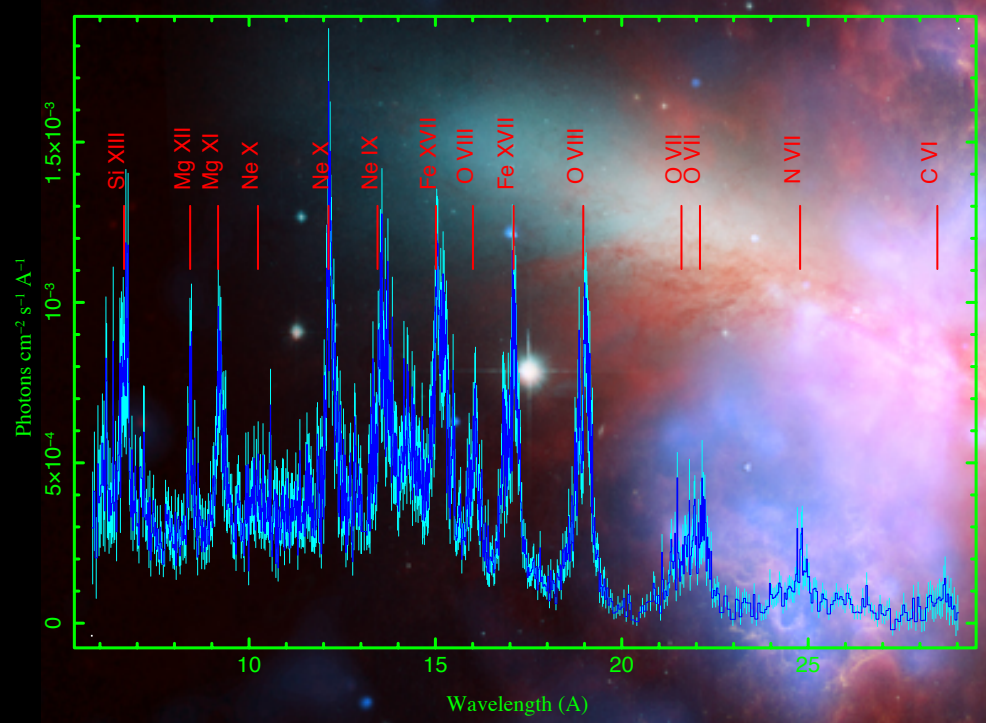

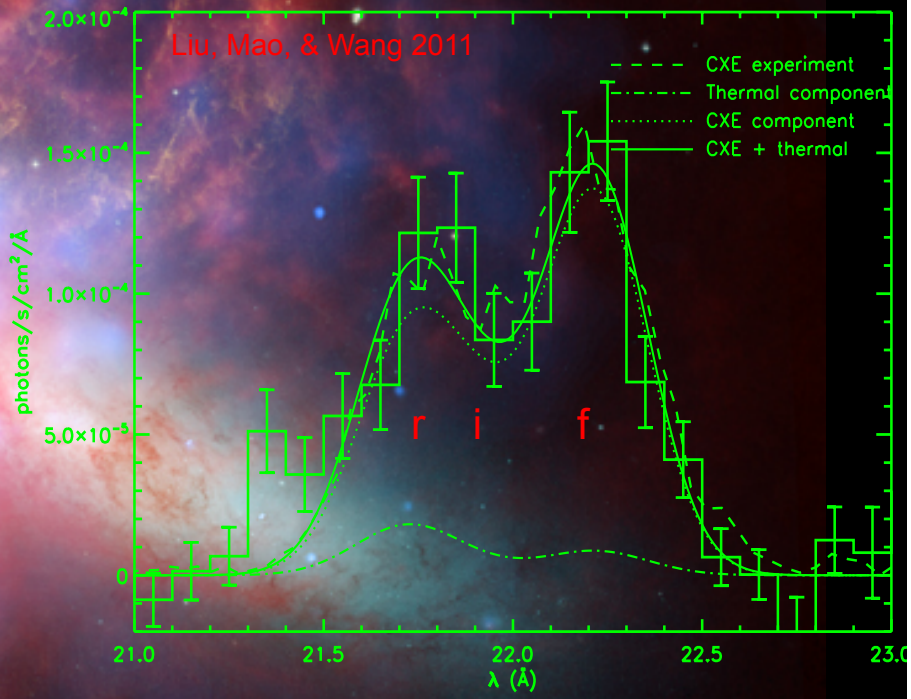

Composite of optical (HST), infrared (Spitzer), and X-ray (Chandra) images

X-ray arises at least partly from the interplay between the hot gas outflow and entrained cool gas clouds, as part of the mass-loading process!

Thermal plasma+charge exchange model Spectral fit to the RGS data of M82

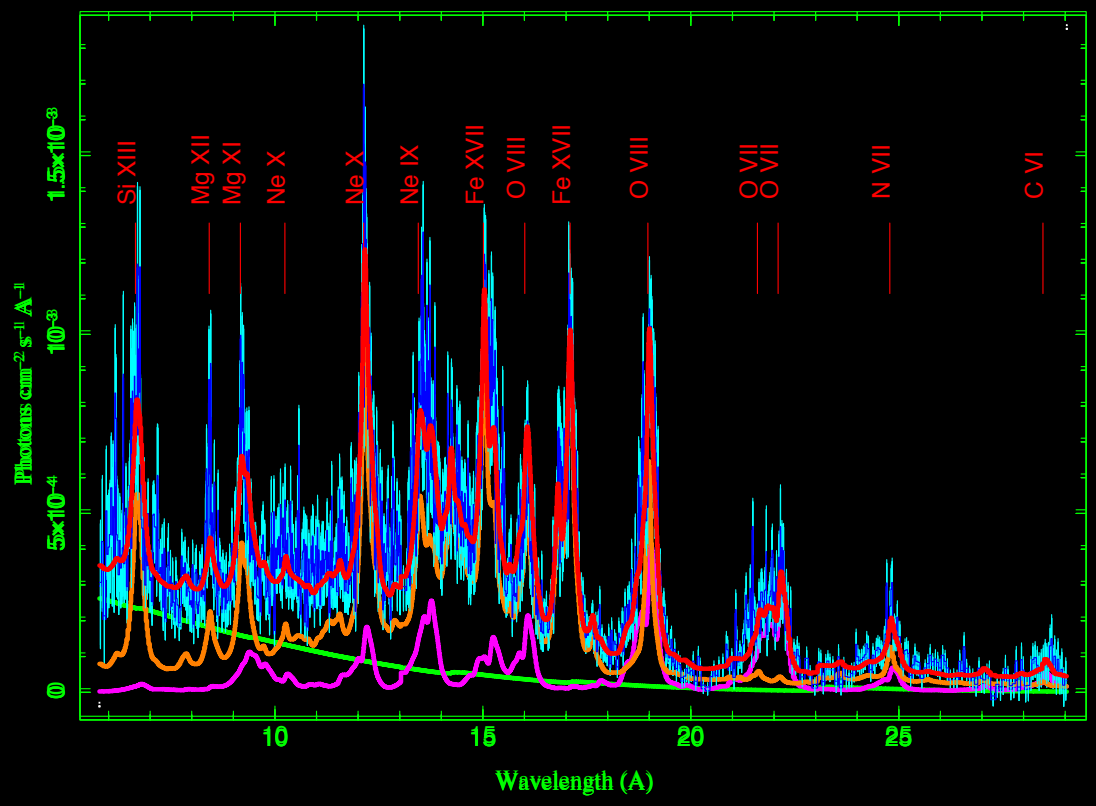

- Naturally explains the spatial correlation between hot and cool gas tracers.
- CX is proportional to the ion flux into the hot/cold gas interface.
- Accounting for the CX is important to determining the thermal and chemical properties of the hot plasma.

Zhang, Wang, Ji, Smith, & Foster (2014)

RGS Survey of nearby active star forming galaxies: examples

Liu, Wang, Mao (2012)

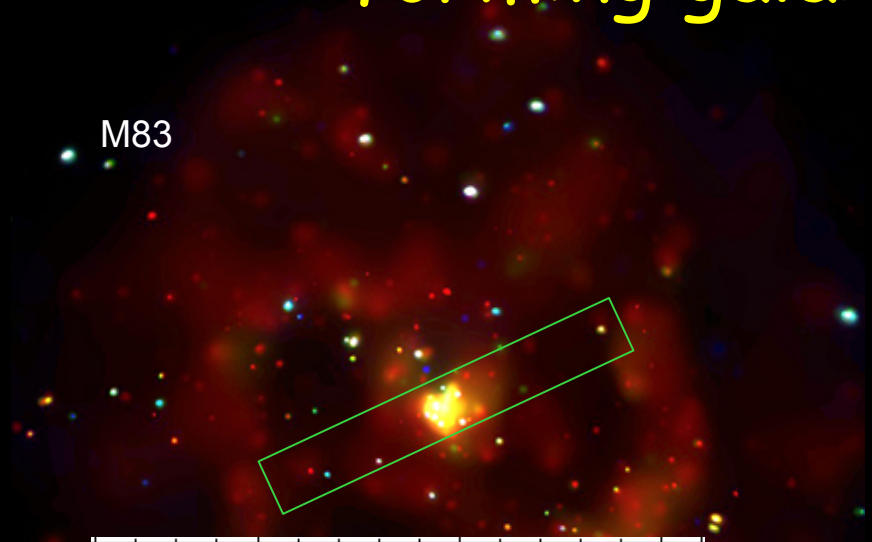

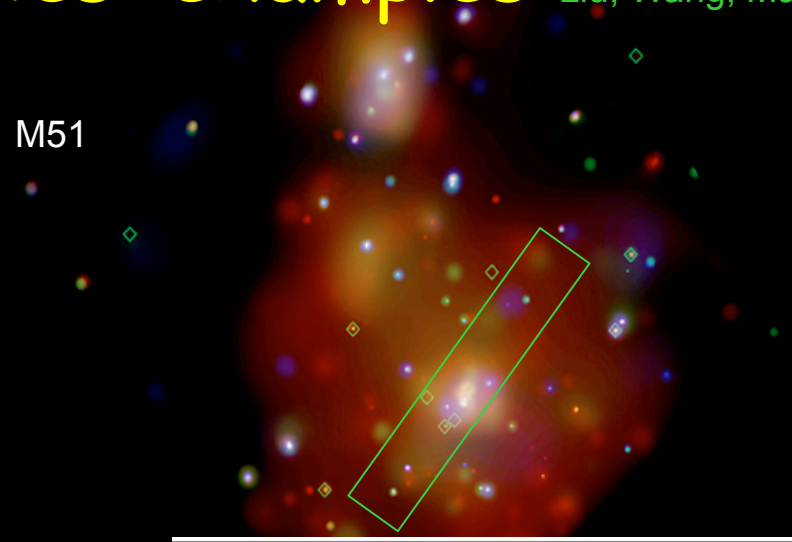

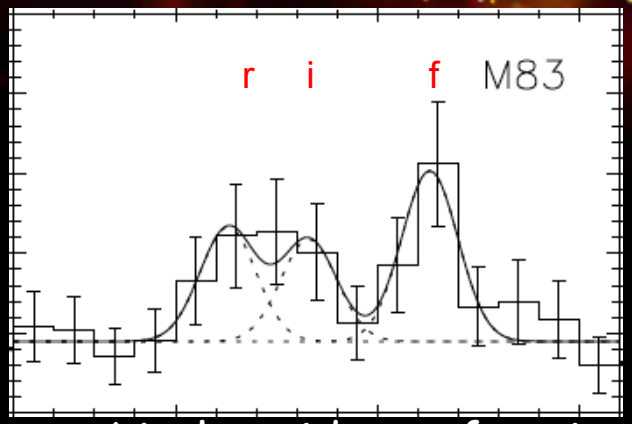

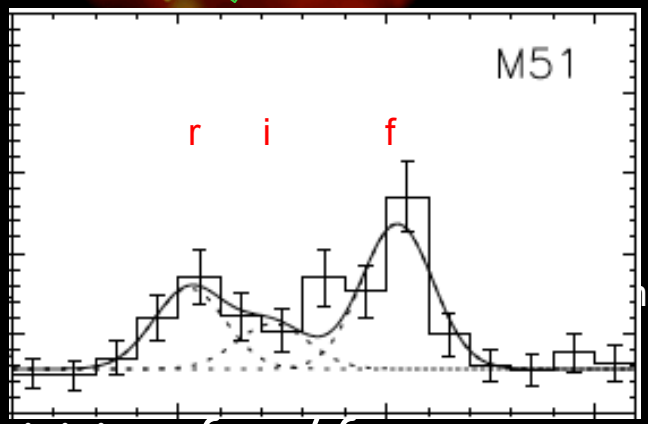

o et al.)

- Little evidence for significant AGN activities; f_{OVIII}/f_{OVII} ratios are similar to star bursts than AGNs
- Soft X-ray are spatially correlated with star forming regions

The diffuse soft X-ray background

Red: ~1/4keV
Green ~ 3/4 keV
Blue ~1.5 keV

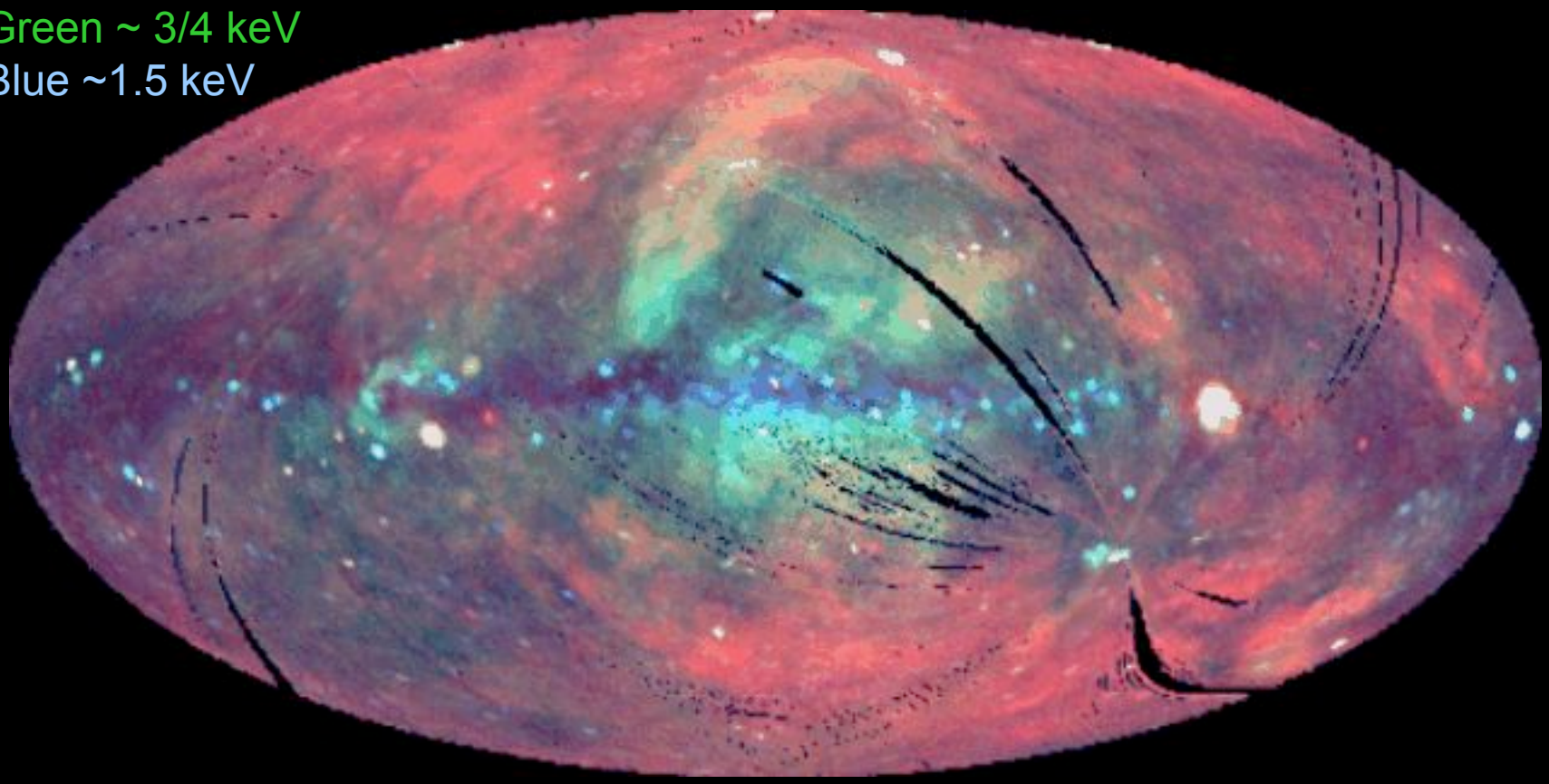

From the Rosat All-Sky Survey

Snowden et al. 1995

Wisconsin sounding rocket ~5 min observation of a lat. region

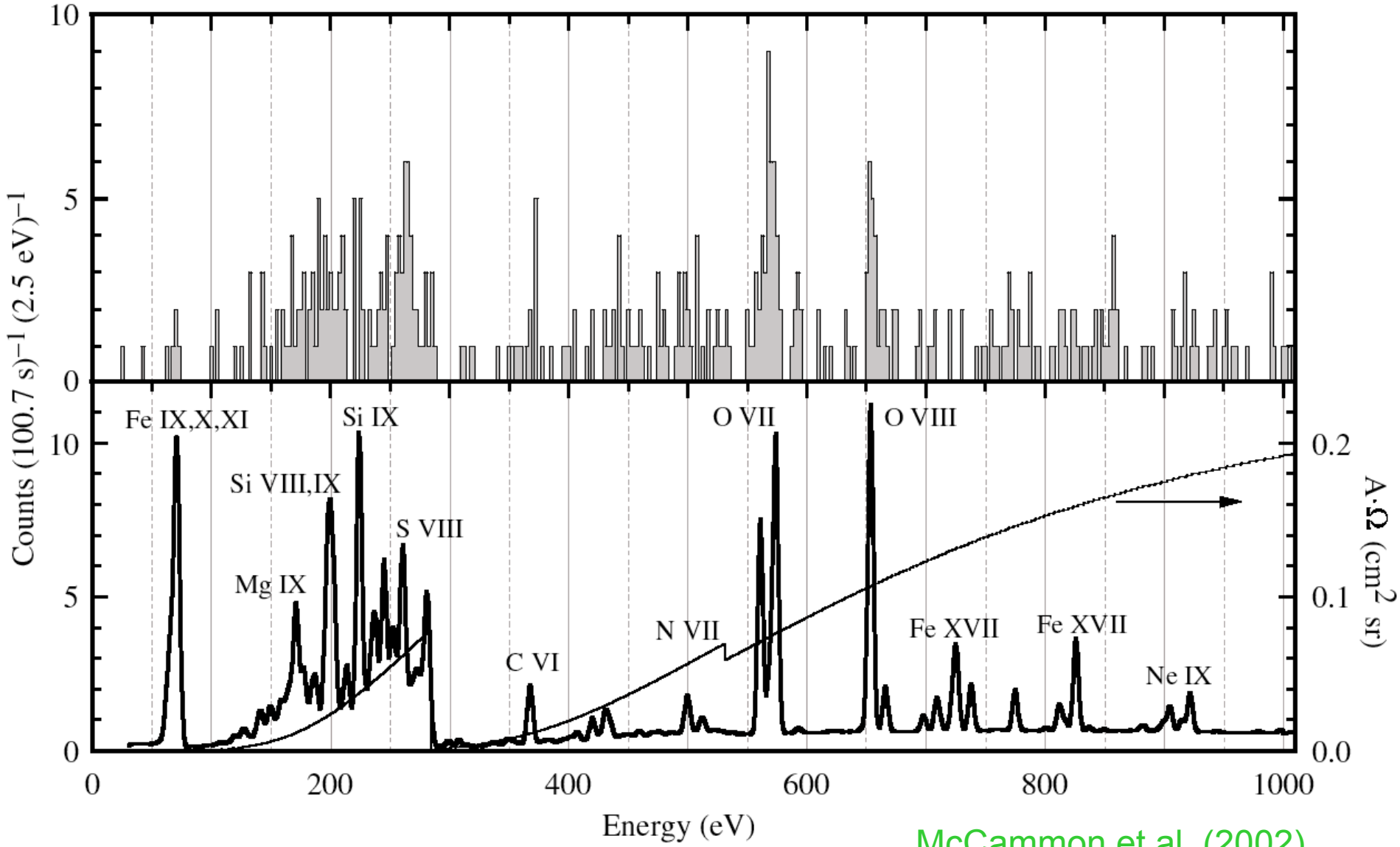

McCammon et al. (2002)

A fraction of the diffuse ¼-keV background arises from SWCX!

- Charge exchange (CX) nature of comet X-ray emission is confirmed, spectroscopically and temporally.
- CX has a cross-section of ~10^{-15} cm^{-2} and occurs on small scales.
- SWCX in the geocorona and within the heliosphere contributes up to ~40% of the ¼-keV background (Galeazzi et al. 2014).
- But the contribution in higher energy bands remains highly clear.

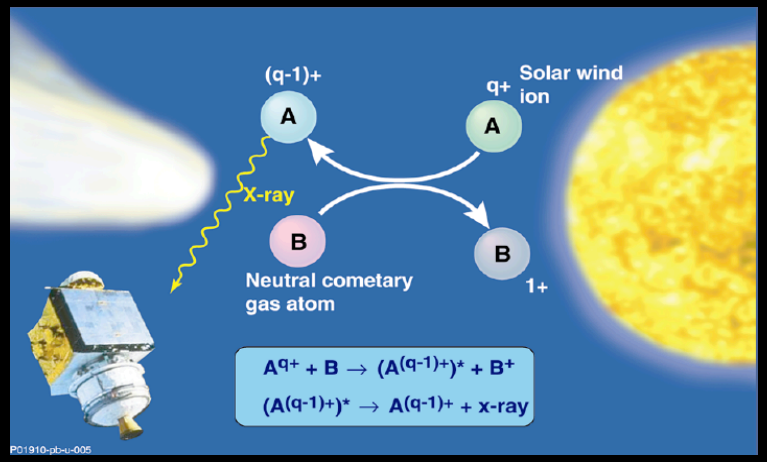

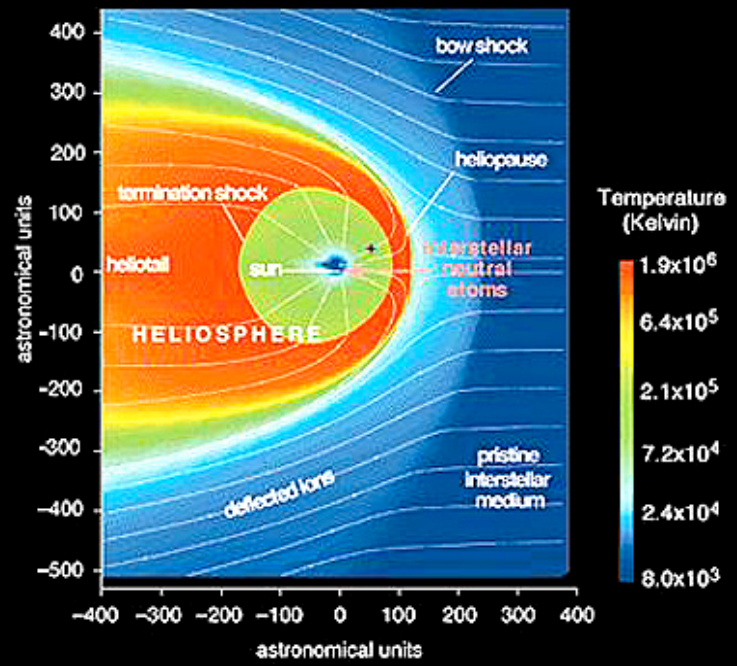

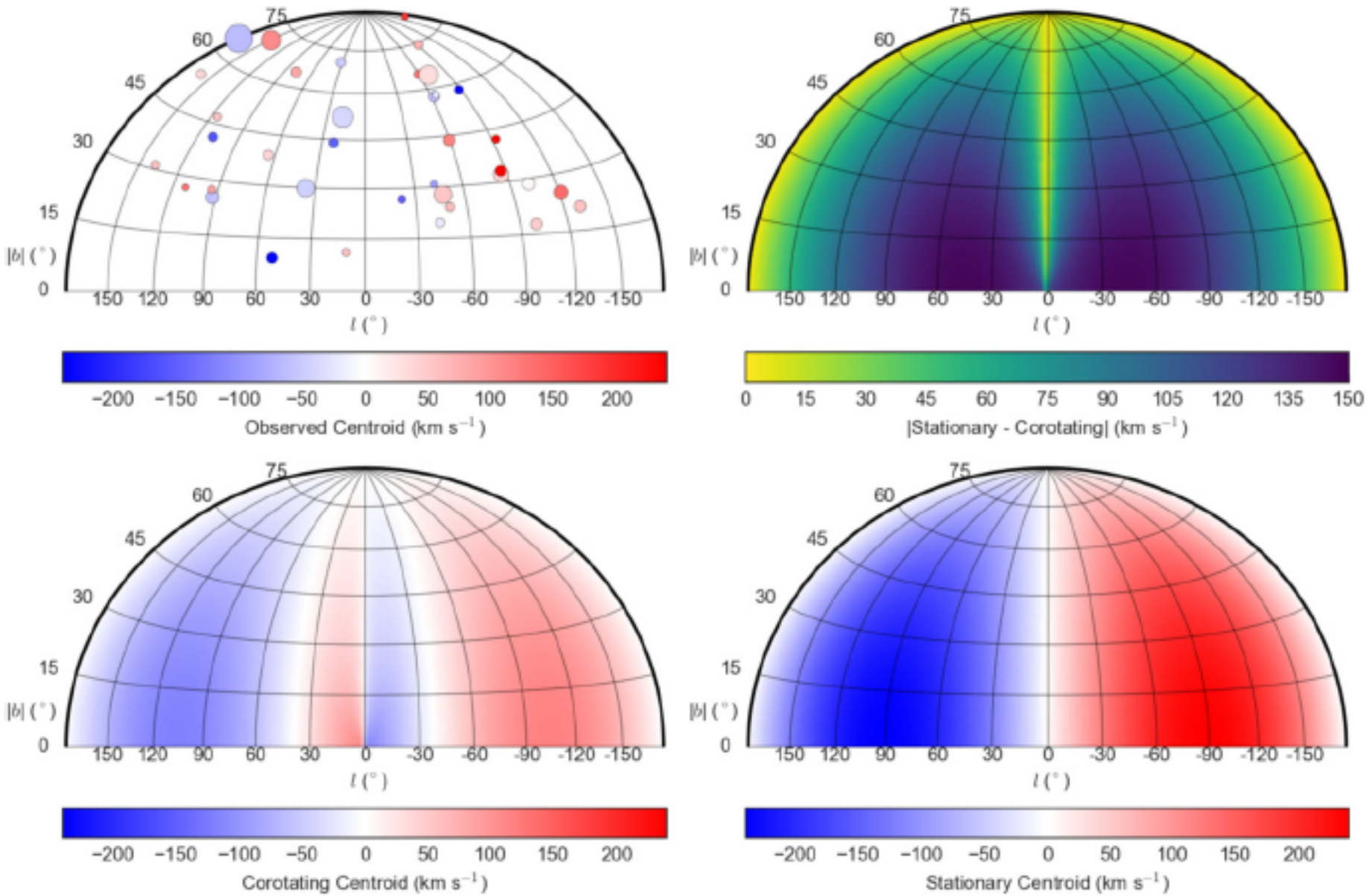

Figure 5. Absorption line centroids in single-hemisphere Aitoff projections. The upper-left panel shows the observed line centroid distribution from Hodges-Kluck et al. (2016) where the point sizes are inversely proportional to their measurement errors. The bottom panels represent model centroid calculations for a cororating (left) and stationary (right) halo gas distribution. The upper-right panel shows the absolute difference between the stationary and corotating model, indicating where on the sky one has the greatest leverage to differentiate between models.

r2f-ratio of OVII Ka

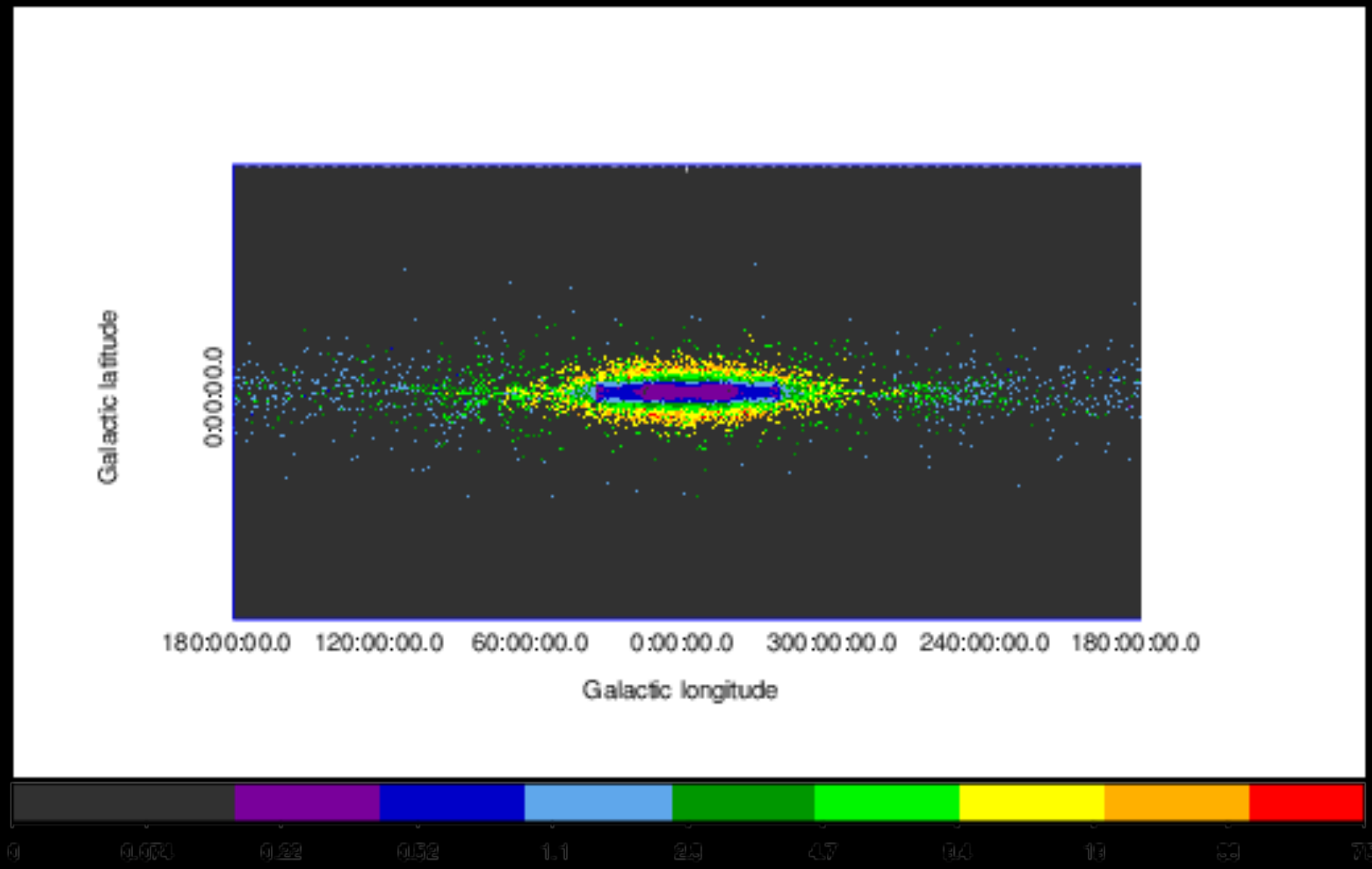

X-ray absorption line spectroscopy is powerful!

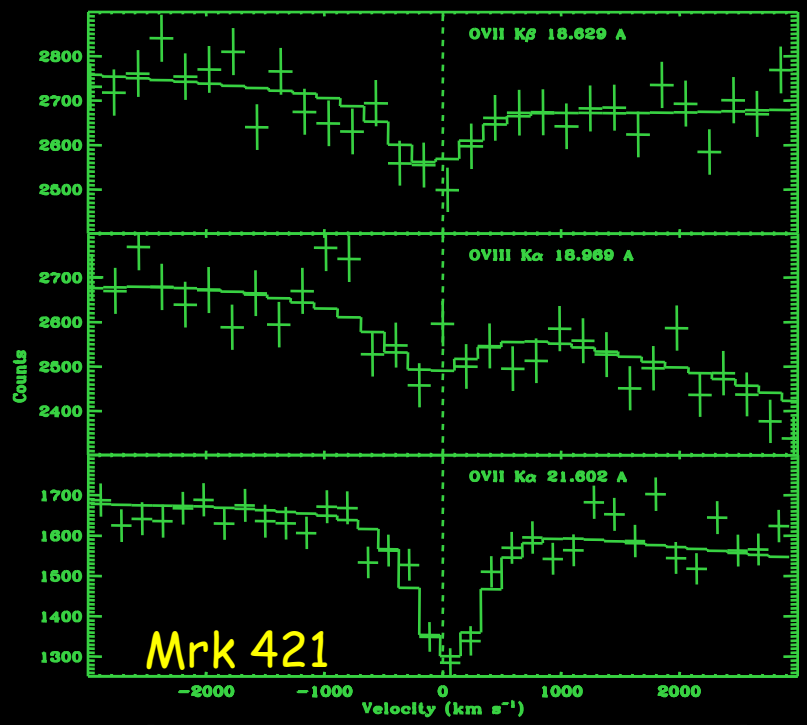

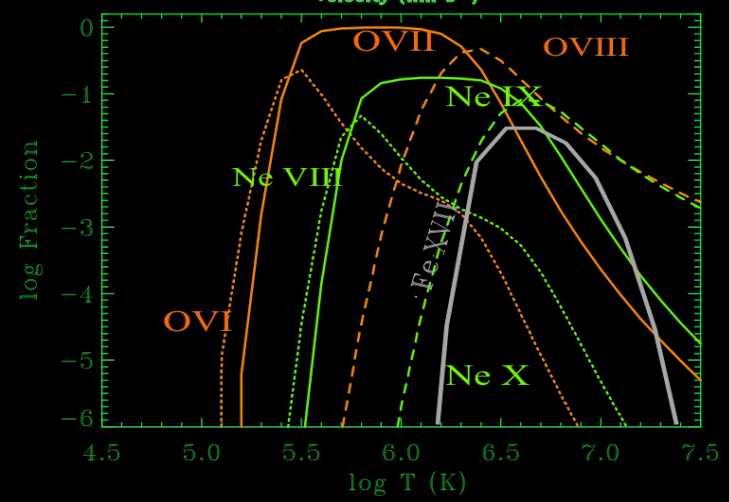

- Tracing all K transitions of metals → all three phases of the ISM.
- Not affected by photo-electric absorption→ unbiased measurements of the global ISM.
- Multiple lines → velocity dispersion, gas temperature, and/or relative metal abundance.
- Multiple sightlines → differential hot plasma properties
- Joint-fit of absorption and emission data → path-length and density

LMC X-3 sightline as an example of X-ray absorption line spectroscopy

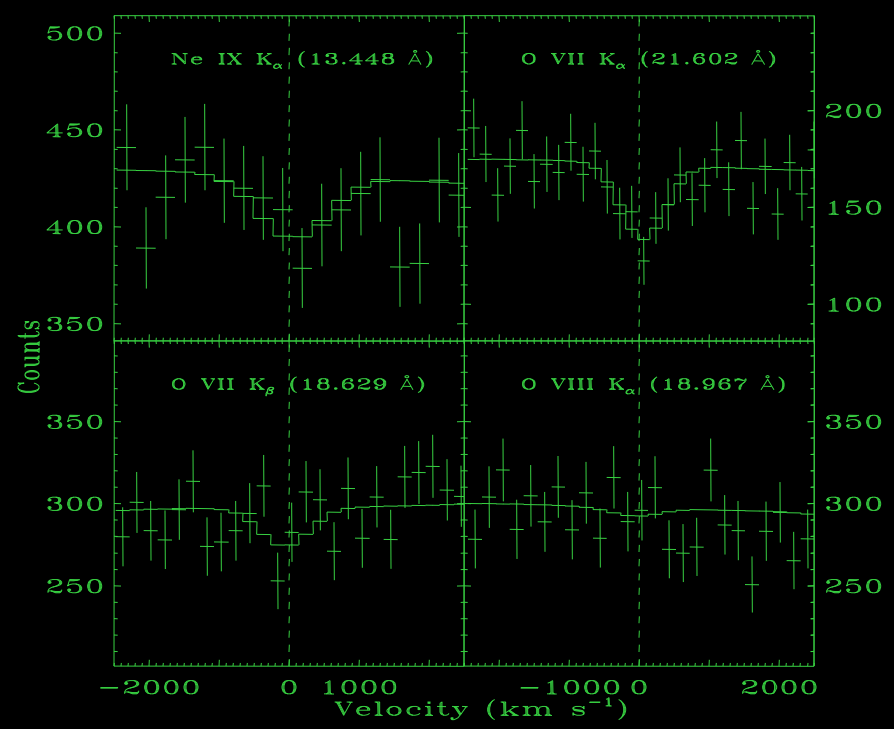

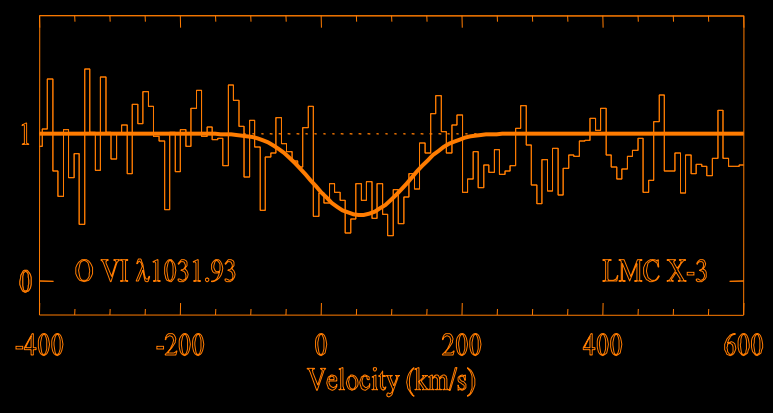

- BH X-ray binary undergoing Roche lobe accretion
- Away from the LMC main body
- 50 kpc away and V_s = +310 km/s
- The line centroids of the OVI and OVII lines are consistent with their Galactic origin.
- $N_{OVII} \sim 1.9 \times 10^{16}$ atoms/cm^2, similar to those seen in AGN spectra!
- b ~ 79 km/s
- T ~ 1.3×10^6 K, lower than that inferred from the emission spectrum of the X-ray background

Wang et al. 2005

OVII Kα line associated with the Sculptor Wall

Toward H 2356-309

N(OVII) ~ 2 x 10^{16} cm^{-2}

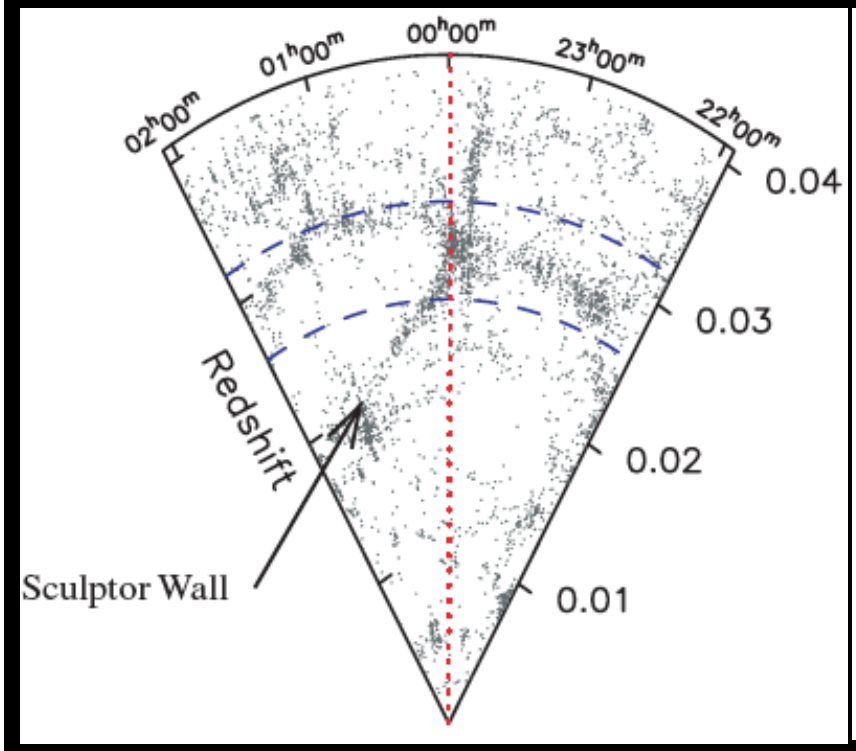

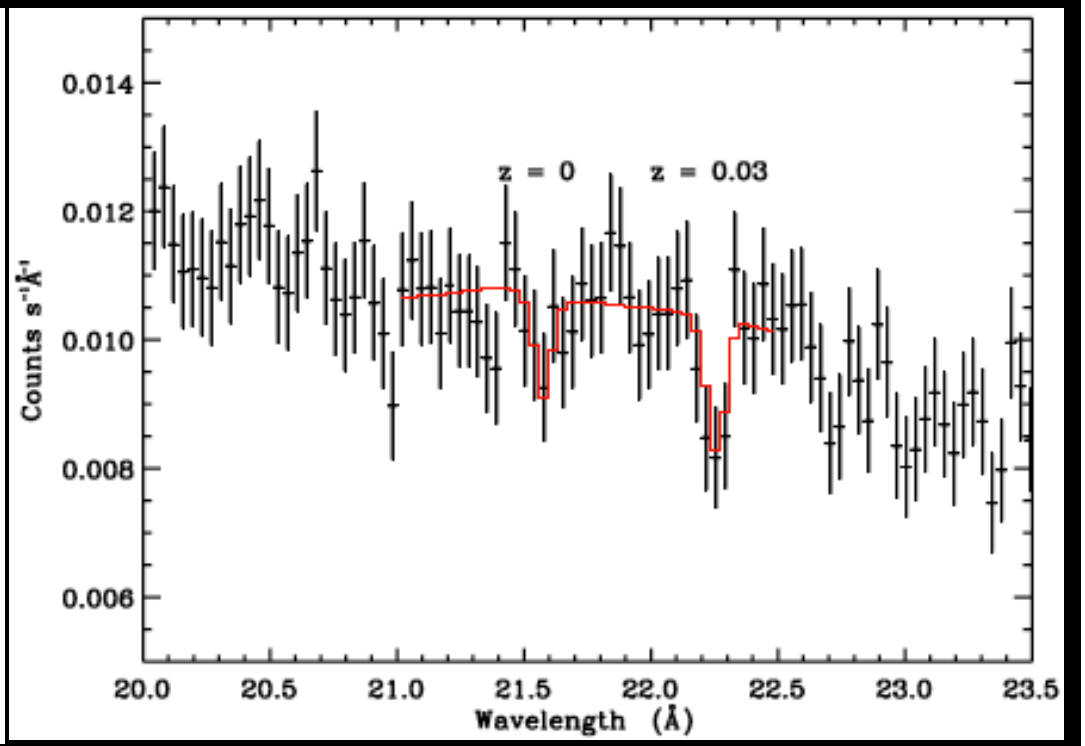

Chandra Grating Data

Buote et al. 2009; Fang et al. 2010

Sample line-of-sight of the COS/halo project

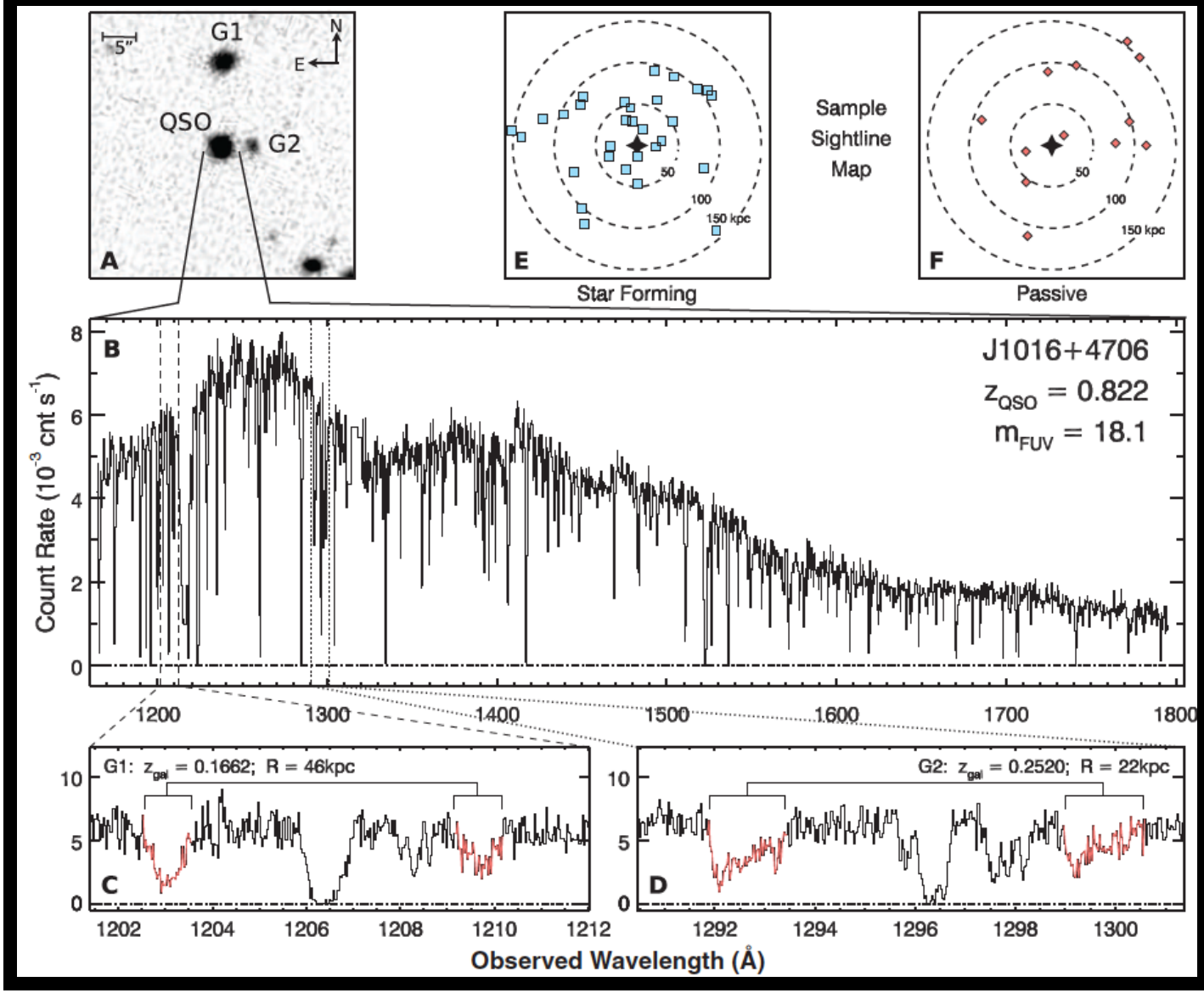

A survey of the CGM of 42 galaxies with the Cosmic Origins Spectrograph onboard the HST.

The detection of redshifted O VI 1032, 1038 Å doublet associated with individual galaxies.

J. Tumlinson et al. 2011

Key results of the COS/Halo project

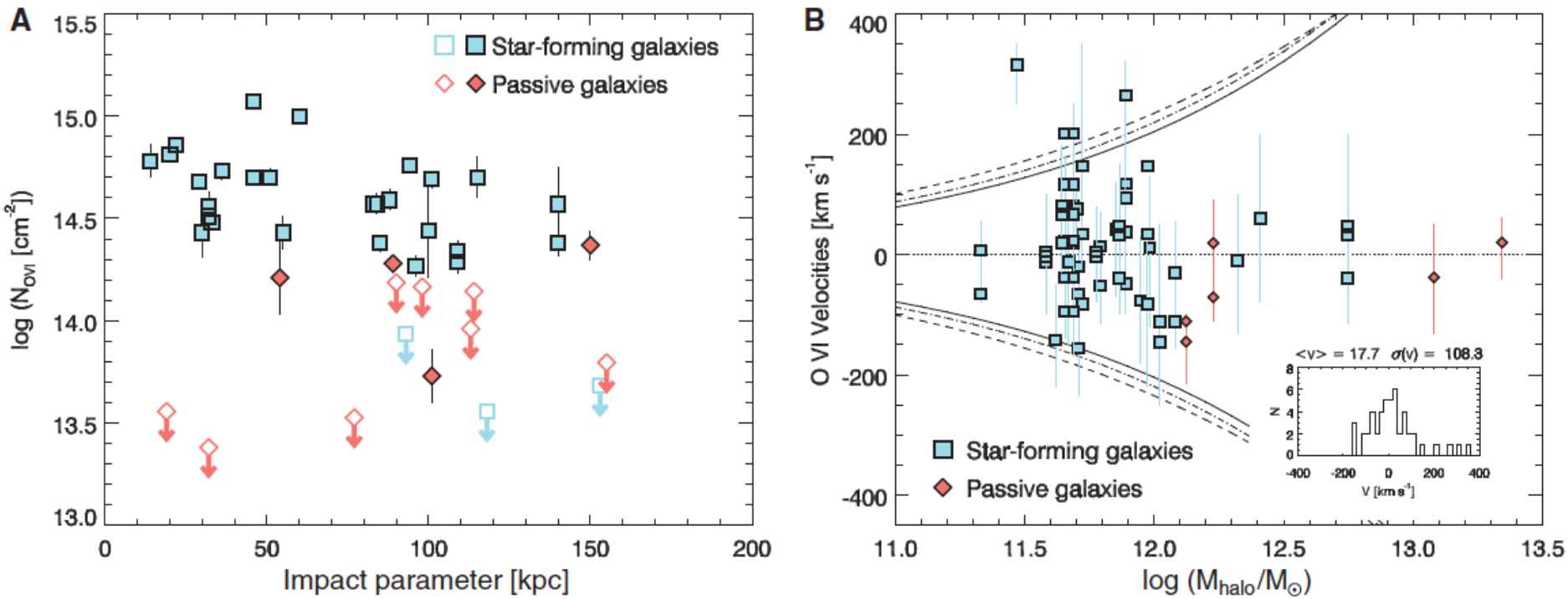

Fig. 2. O VI association with galaxies. (**A**) O VI column density, N_{OVI}, versus R for the star-forming (blue) and passive (red) subsamples. Solid and open symbols mark O VI detections and 3σ upper limits, respectively. The detections in the star-forming galaxies maintain log $N_{OVI} \approx 14.5$ to $R \approx$ 150 kpc, the outer limit of our survey. (**B**) Component centroid velocities with respect to galaxy systemic redshift for O VI detections, versus inferred dark-matter halo mass. The range bars mark the full range of O VI absorption for each system. The inset shows a histogram of the component velocities. The dashed lines mark the mass-dependent escape velocity at R = 50, 100, and 150 kpc from outside to inside.

Generalizing the typical M_{OVI} to all star-forming galaxies with $M^* > 10^{9.5}$ $M_{\odot}$ → Such OVI absorbers contain ~15% ($0.02/f_{OVI}$) of the oxygen and 2%($0.02/f_{OVI}$) ($Z_{\odot}/Z$) of the baryons in the universe. But the nature of the absorbers remains highly uncertain! Their filling factor is small.

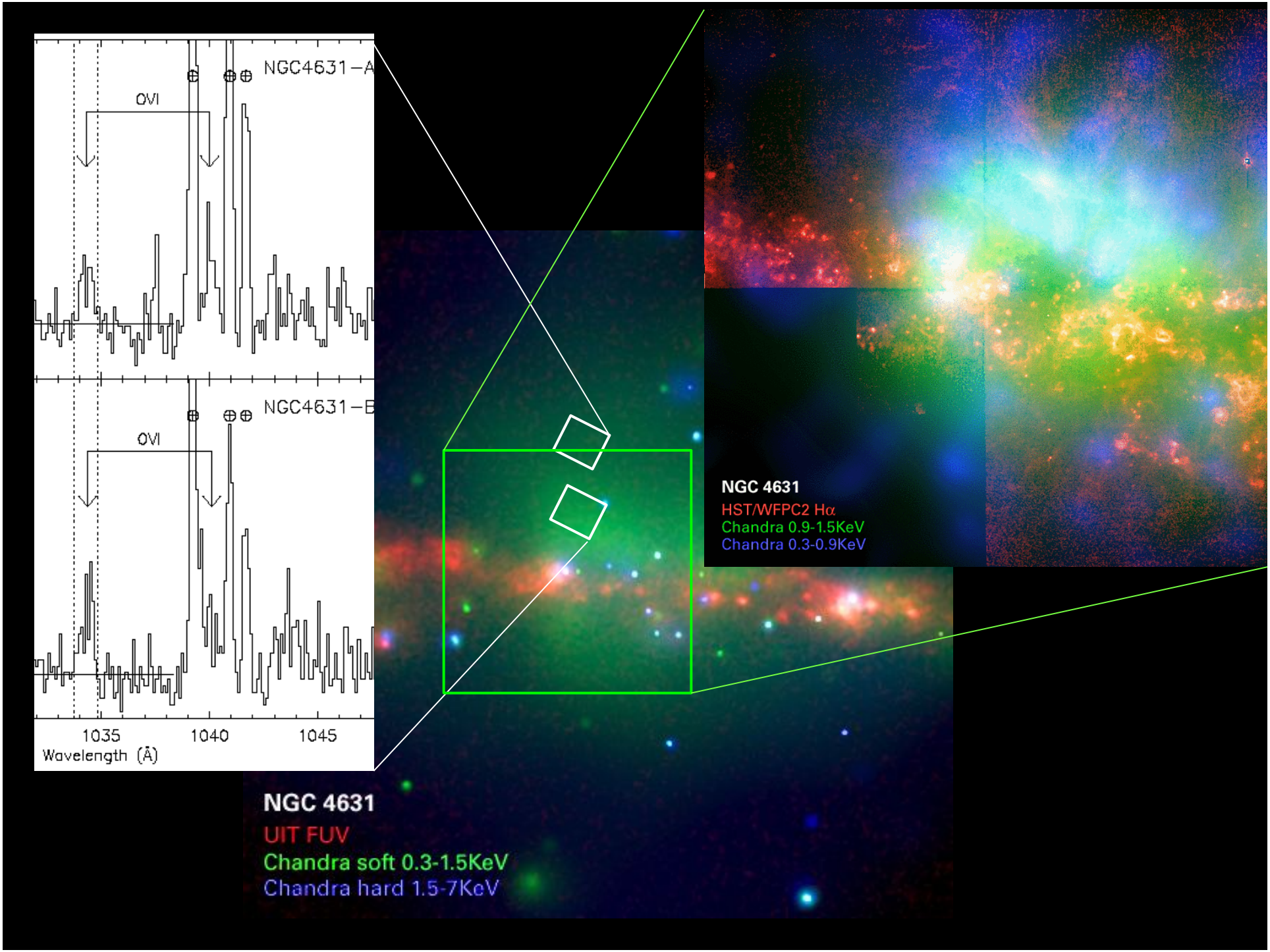
NGC4631−A
OVI
NGC4631−B
OVI
1035
1040
1045
Wavelength (Å)
NGC 4631
HST/WFPC2 Hα
Chandra 0.9-1.5KeV
Chandra 0.3-0.9KeV
NGC 4631
UIT FUV
Chandra soft 0.3-1.5KeV
Chandra hard 1.5-7KeV

First HST-ACS/SBC image of OVI emission from a starburst galaxy

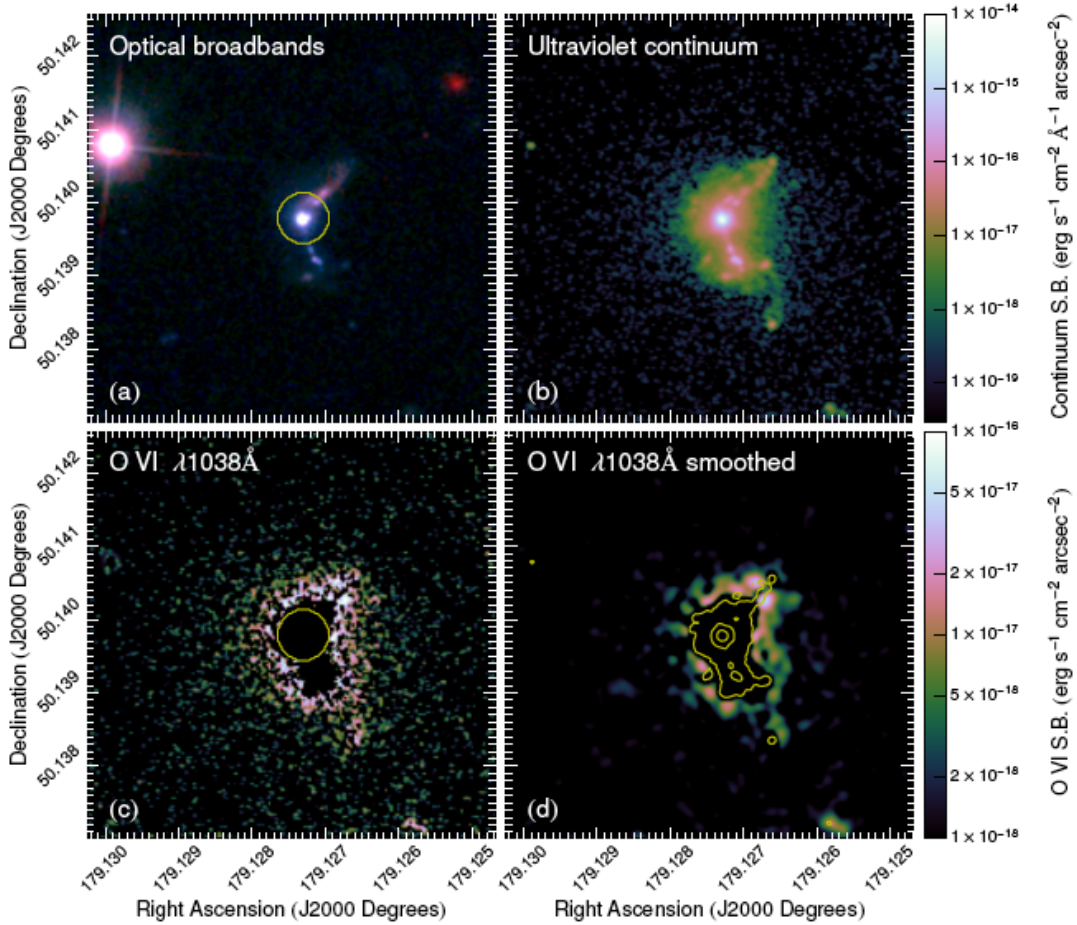

- DSSJ115630.63+500822.1
- D=1200 Mpc (z = 0:235)
- star formation rate ~40 times higher than the Milky Way (40 M yr^{-1})
- selected to maximize the chances of detecting O vi emission.
- a net equivalent width of a few tenths of an Å, compared to the bandpass of ~ 100 Å.

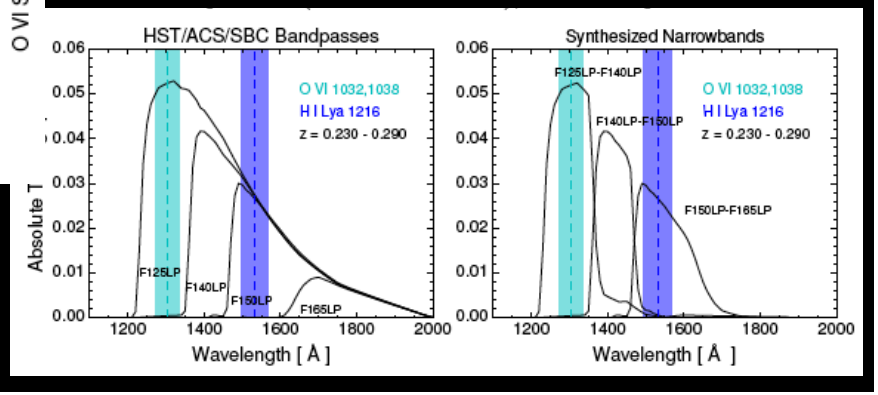

Hayes et al. 16

COS Spectrum toward a star cluster

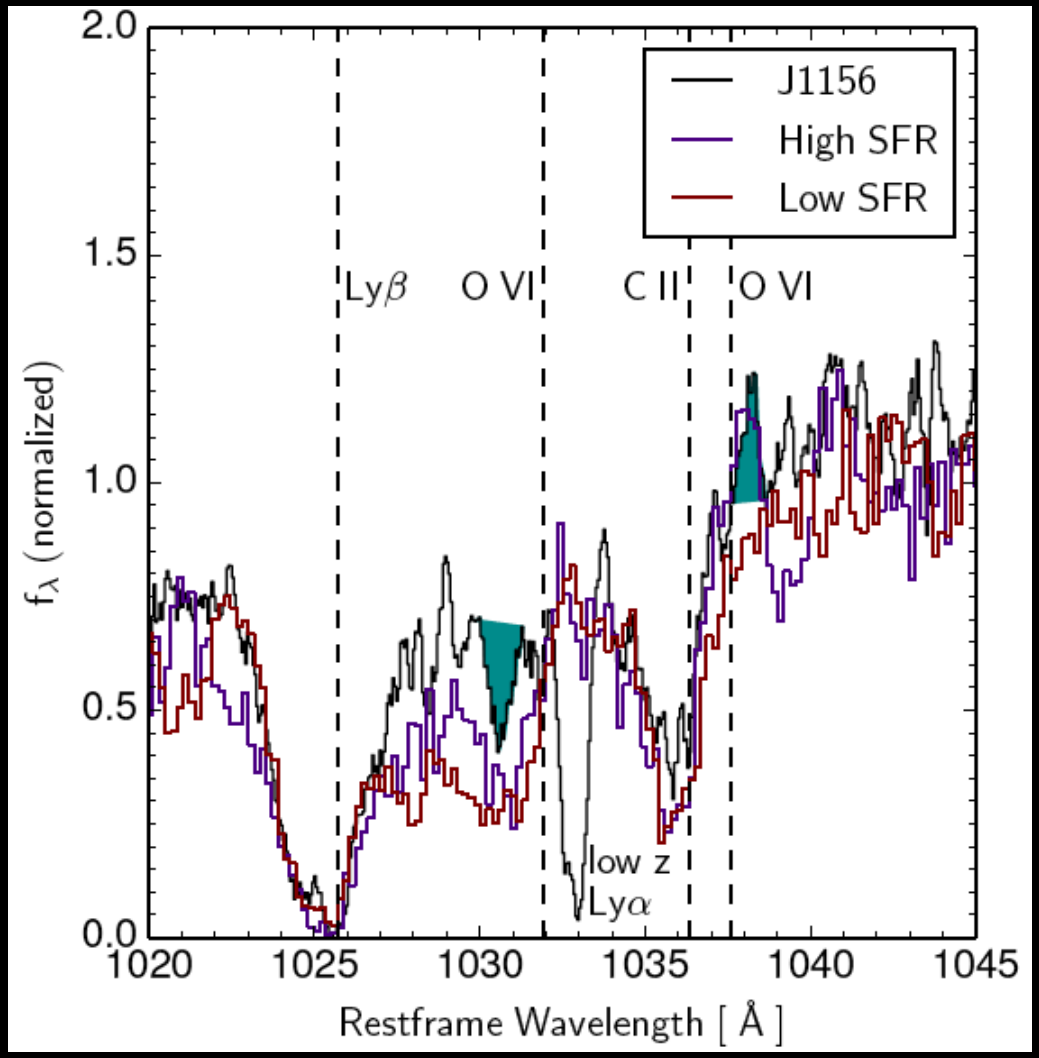

2.5-arcsecond diameter circular aperture, which was centered upon the UV dominant star cluster.

Spectra of strongly and weakly star-forming galaxies are shown in purple and red (Heckman et al. 2011; Henry et al. 2015).

Detecting ~10^7 K in far-UV

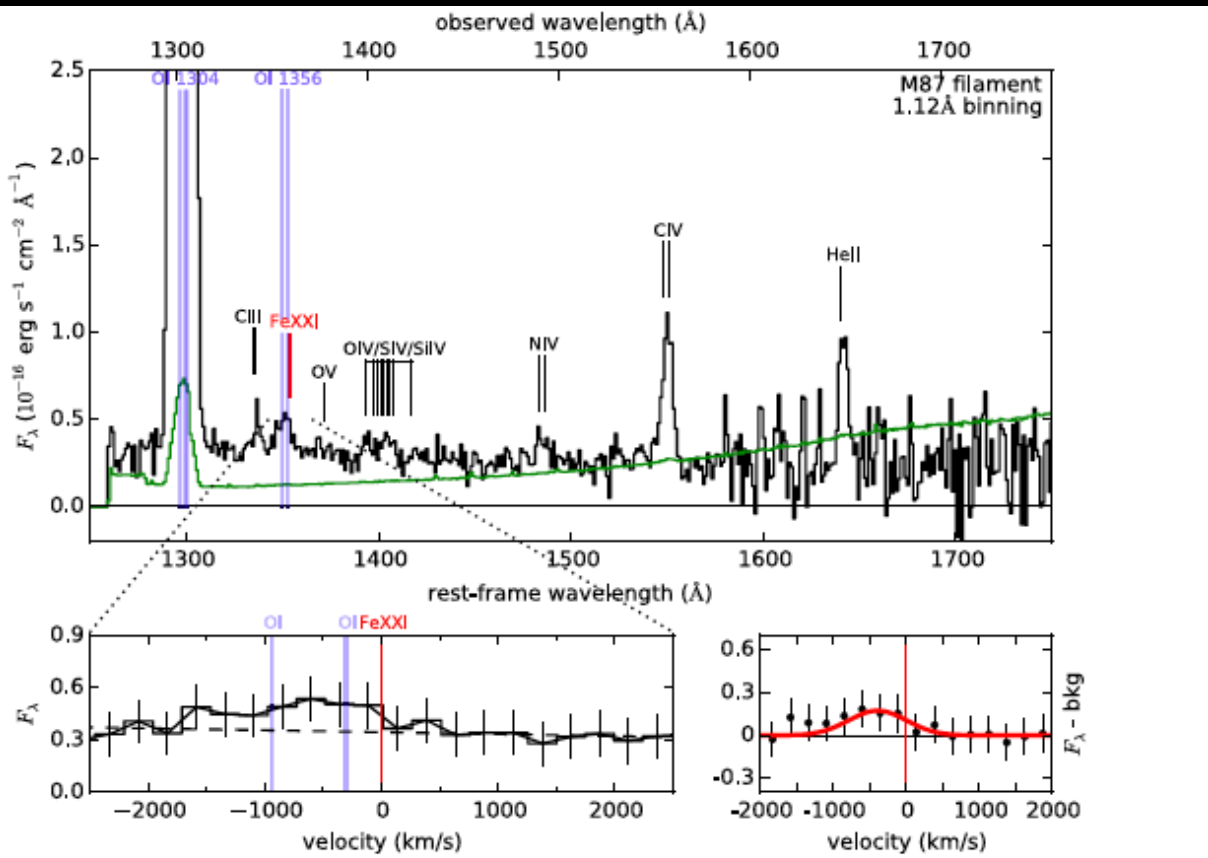

Figure 3. (top) Average spectrum of COS G140L observations of a filament projected 1.9 kpc from the nucleus of M87. Unlike the previous figure, we have not restricted this spectrum to the night-only observations; O I λ1304 airglow is therefore extremely prominent, but we argue that the feature near O I λ1356 is probably [Fe XXI], with a negligible airglow contribution. The feature is significant at 2.2σ.

ground-state magnetic dipoleTransitions

Anderson and Sunyaev 16

High spec res.

When better observed, allowing for measurements of bulk and turbulent motion

When combined with other observations, providing constraints on the cooling process.

Summary

- The weakest link in the cosmic structure formation theory is our poor understanding of the baryon physics.
- The most sensitive spectroscopic diagnostics of the physics are in Far-UV and soft X-ray.
- Existing very limited observing capabilities in these wavelength bands have been explored, demonstrating the power of the spectroscopy.
- However, various important phenomena and physical processes are yet to be investigated.
- We badly need data from far-UV and X-ray IFU-type spectrometers, ideally in a joint mission, allowing for simultaneous far-UV/X-ray spectroscopy of absorption and emission lines.

Cosmic Baryon Surveyor

- Complete the cosmic inventory of the baryon matter in various phases
  - Thermal, chemical, and dynamic properties, as well as the location and content inventory.
- Understand the baryon physics governing the structure formation
  - Heating and/or cooling mechanisms
  - Energetics of the inflow and outflow in and around galaxies
  - Microscopic physics and radiation mechanism at hot/cool gas interfaces
- Measure AGN feedback
  - Mass and energy rates of outflows
  - Episodic behavior and effect on surrounding medium (from small to large scales).
- Serve as a general observatory
  - Solar activity and wind, heliosphere, comets and planets, stars, …

Normalized absorption profiles from the STIS and FUSE spectra of Mrk 279

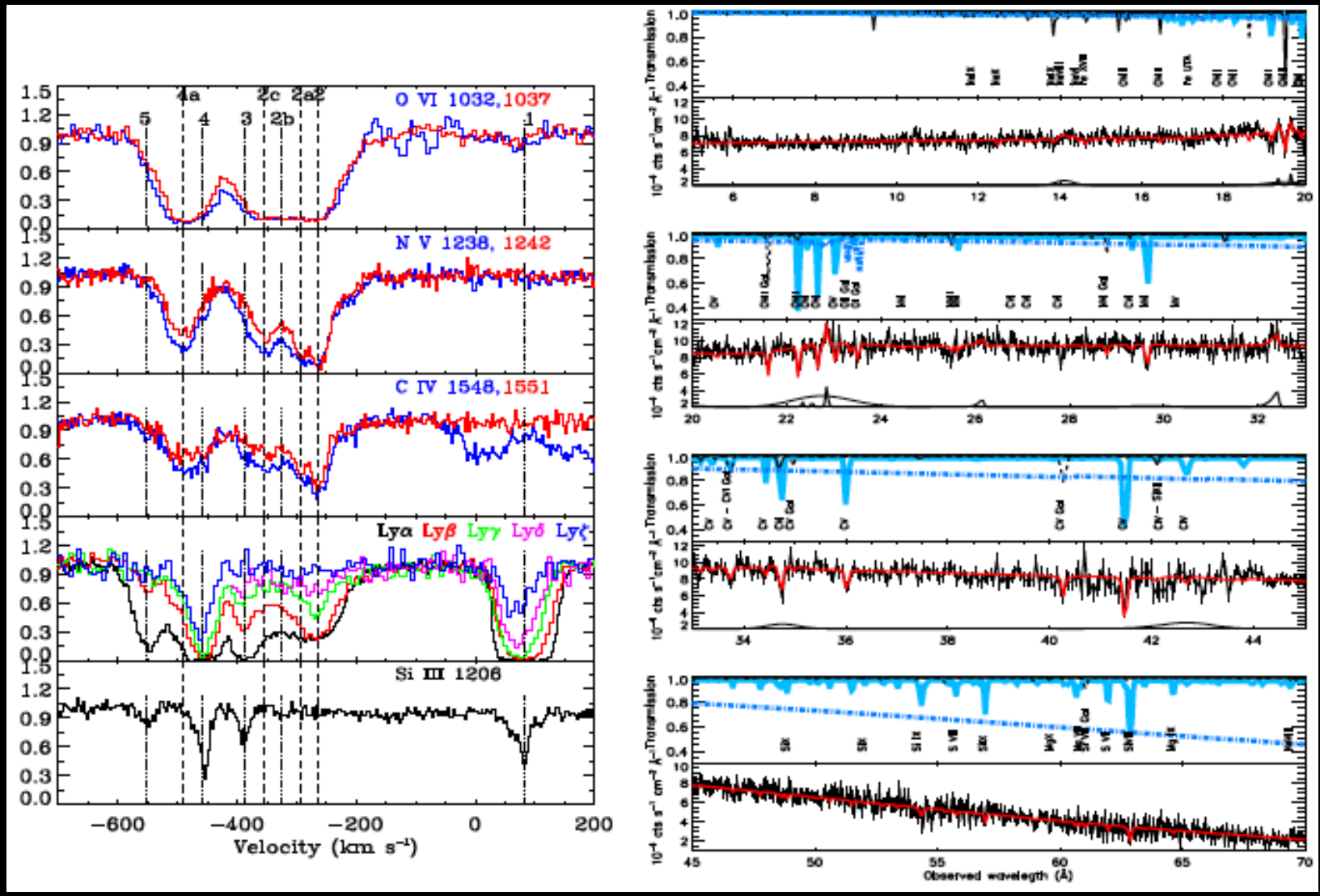

Costantini 2010

Why emission lines?

- In the paper "**How the diffuse Universe cools**", Bertone, Aguirre & Schaye (2013) reached the conclusion "It would therefore be highly desirable to build a satellite with the capability to try to detect emission at high spectral resolution in the FUV band *of* ~ 100–1000 Å, where most of the strongest emission lines and a large fraction of the continuum emission are found."
- dominated by high-density regions (proportional to n^2) , particularly sensitive to the ISM/IGM/ICM.
- complement absorption line studies (proportional to N), allowing for inference of the density and l.o.s scale.
- providing a 2-D image, in addition to the velocity of the emission line, allowing for the study of 3-D spatial distribution.
- Detection of non-resonance lines, often useful for critical diagnostics of underlying physical processes.

Why high spectral resolution?

- Sensitive and clean measurements of individual lines with minimum noise from the continuum and line blending.
- Measurement of the continuum emission (electron bremstrahlung), particularly important for absolute abundance estimates
- 1 eV corresponds to ~500 km/s at 0.6 keV, or 7 Mpc in the Hubble flow.
- allowing for absorption line spectroscopy, even kinematics of bulk motion (galactic rotation, outflows driven by SB and/or AGN).

Providing diagnostics key to the understanding of astrophysics of the structure formation

- Various powerful line diagnostics
  - doublet (Li-like; e.g., OVI)
  - triplet (He-like; OVII)
  - Multiple (Ne-like; Fe XVII)
- Sensitive to key physical processes:
  - Collisional excitation
  - Photo-excitation
  - Non-ionization equilibrium
  - Resonance scattering
  - Charge exchange at cool-hot interfaces

Key questions that can be potentially addressed

- Where are the baryons? How important is photoionization in producing the IGM O VI seen in absorption? How important is non-equilibrium physics? Is the brightness distribution of knots in the WHIM consistent with cosmic web models?
- What is the distribution of the warm and transition temperature gas in the CGM? How does the CGM cool and enter galaxies?
- Where are the metals? Are they found inside or outside of galaxies?
- What is the pressure of hot gas in the Galactic halo? How much supernova energy is dissipated in the Milky Way? How is the hot gas in the Galactic disk distributed?

2010 US decadal report states

"A new and potentially ground-breaking area of study consists of mapping the metal and hydrogen-line emission from circumgalactic and dense filamentary intergalactic gas, using IFUs in the UV. Such observations will provide direct information about the kinematics, density, and chemical content of baryons cycling between galaxies and the IGM."

In addition to the recommendation of the Athena-like calorimeter X-ray mission.

Soft X-ray line emission from simulated halos at $z = 0.125$

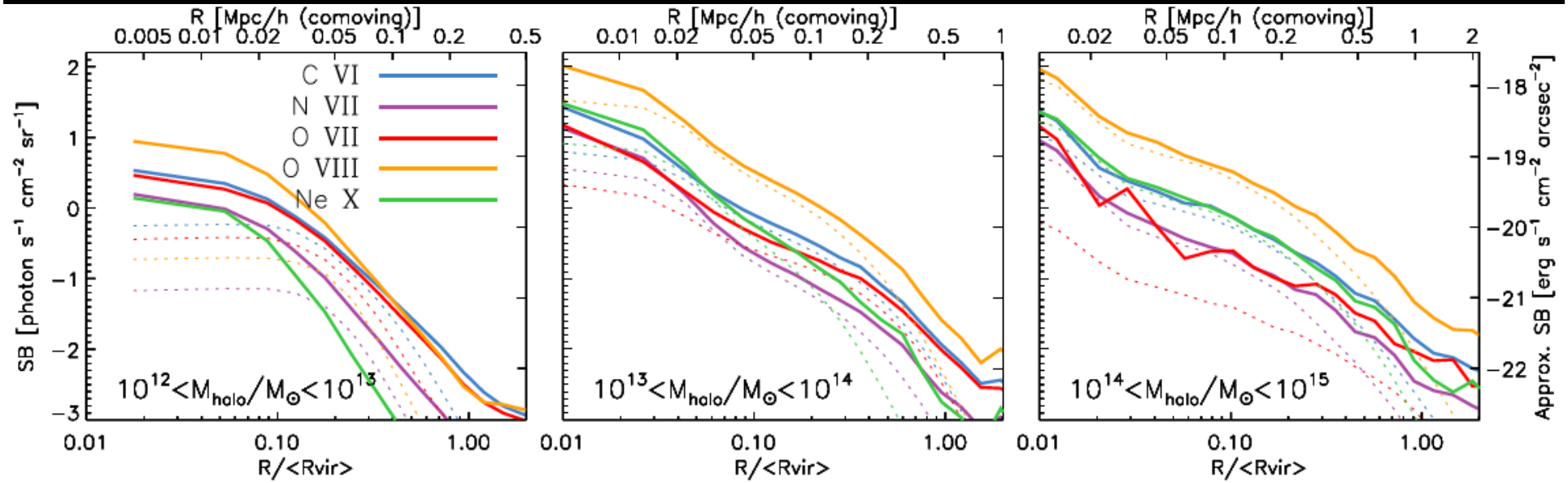

b

van de Voort & Schaye (2013)

UV/optical line emission from simulated halos at $z = 0.125$

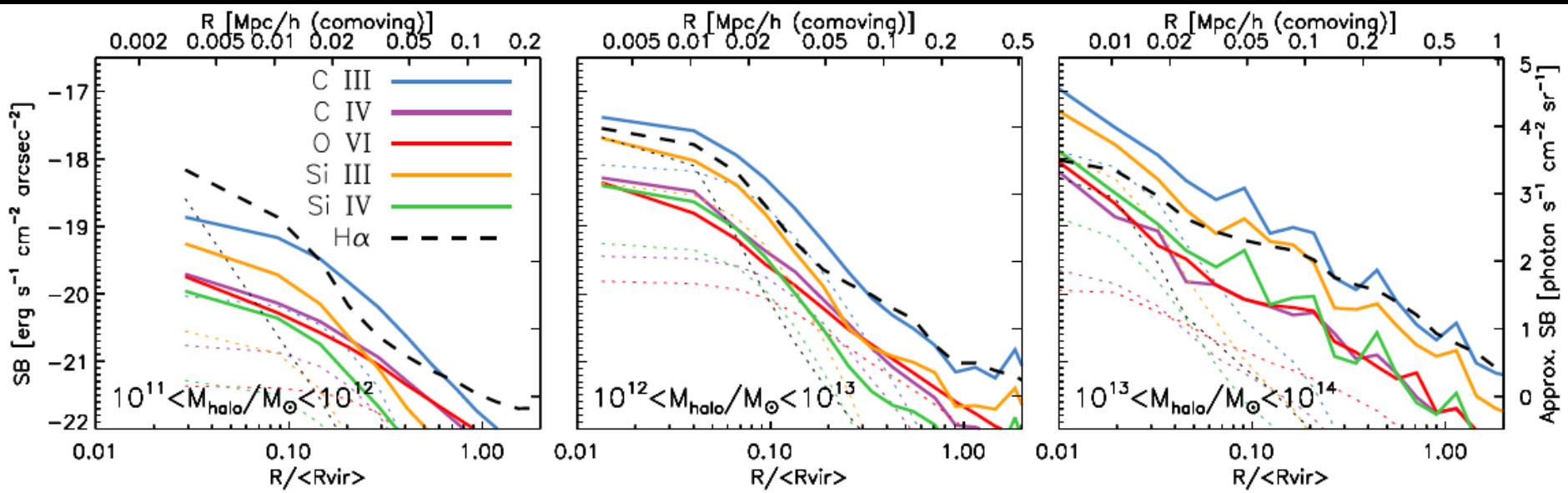

b

CX emission as the probe of cold flows around galaxies: H may be largely ionized. CX may mostly be carried with HeII. Could the existing simulations be used to make estimates?

Recombining plasma around dead quasar:
X-ray spectral line diagnostics of various physical processes:
Key line ratios:
OVII Ka r/f
OVIII/OVII Ka(not good if there is a temperature distribution)

Kgamma/Kbeta/Kalpha of OVII and OVIII
processes:
Thermal CIE
- isothermal as a function of kT
- isobaric or isochroric cooling

Non-CIE cooling and heating
Photo-ionized plasma
- equiribrium plasma as a function of the ionization parameter, etc.
- relic plasma

Charge exchange
Resonance scatter

- HUBS, we are now aiming at an energy resolution of 2 eV for emission lines and < 1 eV for absorption lines, along with a modest spatial resolution of 3′, 1 deg^2 FoV, and 600-1000 cm^2 effective area.

Known unknowns of the hot gas

- Overall extent, as well as the density, temperature, and metallicity structures of the potential large-scale hot gaseous halo, let alone its mass.
- Vertical temperature structure of the thick hot gas disk, even qualitatively.
- Detailed velocity structure.
- Ionization state, as well as the charge exchange contamination and resonance scattering of key emission lines.
- The decomposition of the various hot gas components remain highly model-dependent!

- Microcalorimeters of a given design normally have ~constant ΔE.

- But if designed for a lower maximum energy then $\Delta E \propto$ ~sqrt(E_{MAX})

- Smaller detectors can have better energy resolution.

- Approximate best current results:

ΔE ~25 eV at 100 keV

ΔE ~1.6 eV at 6 keV

ΔE ~0.8 eV at 1.5 keV

ΔE ~0.1 eV at 5 eV

Looking for the Missing Baryons

Redshift can separate weak lines of WHIM filament from bright Galactic foreground emission:

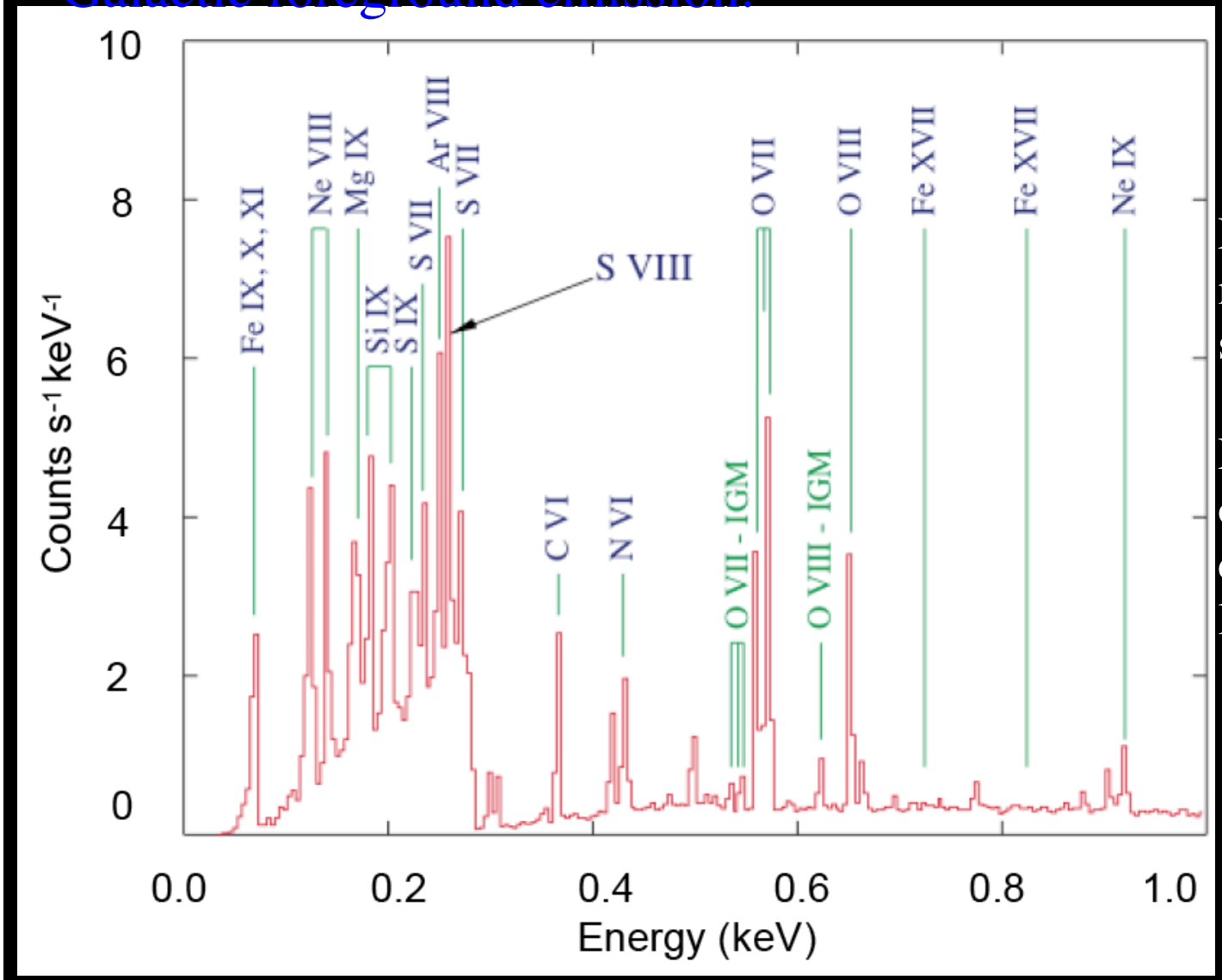

Need emission measurements to map structure.

Need absorption line observations to detect cooler WHIM gas at lower temperatures.

The mass-weighted distribution of cosmic diffuse gas

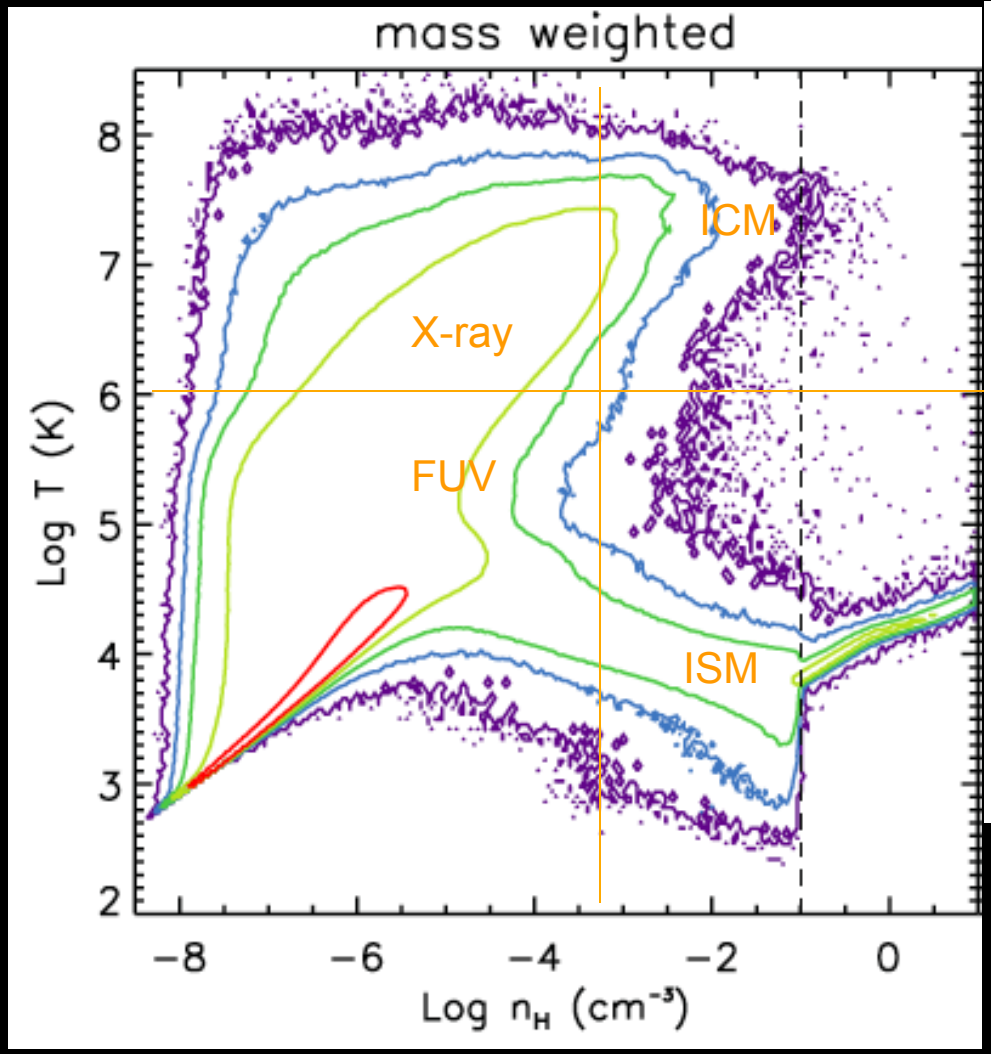

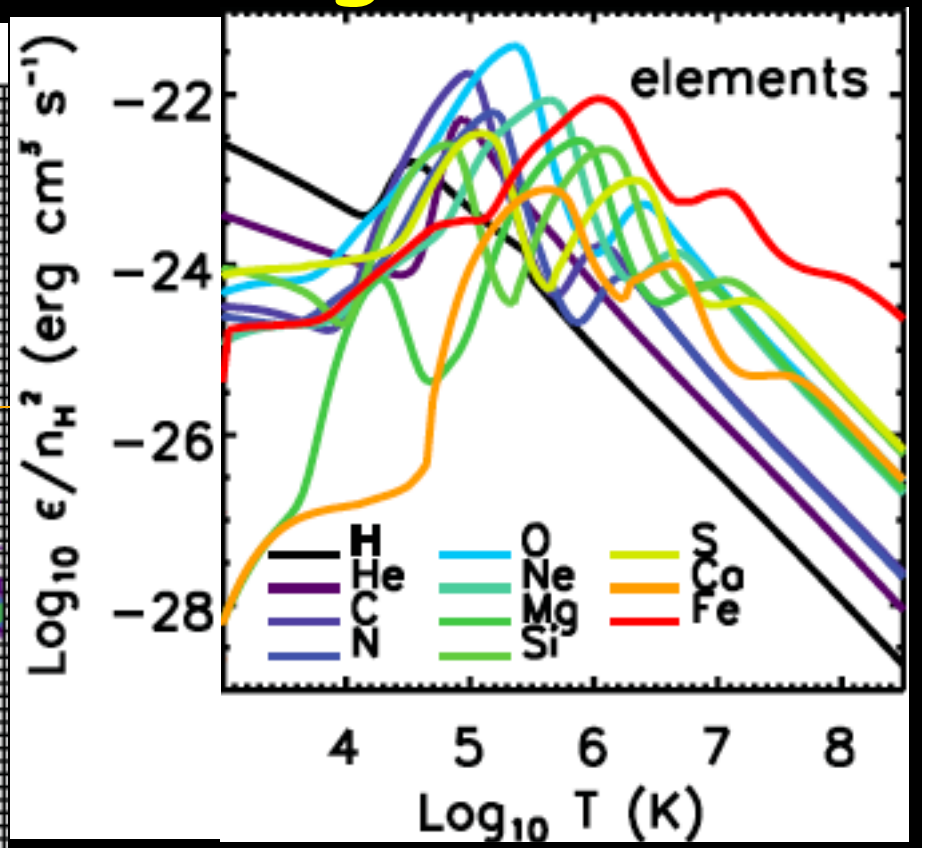

total line emissivity of each element (assuming solar abundances.

S. Bertone, A. Aguirre and J. Schaye (2013)

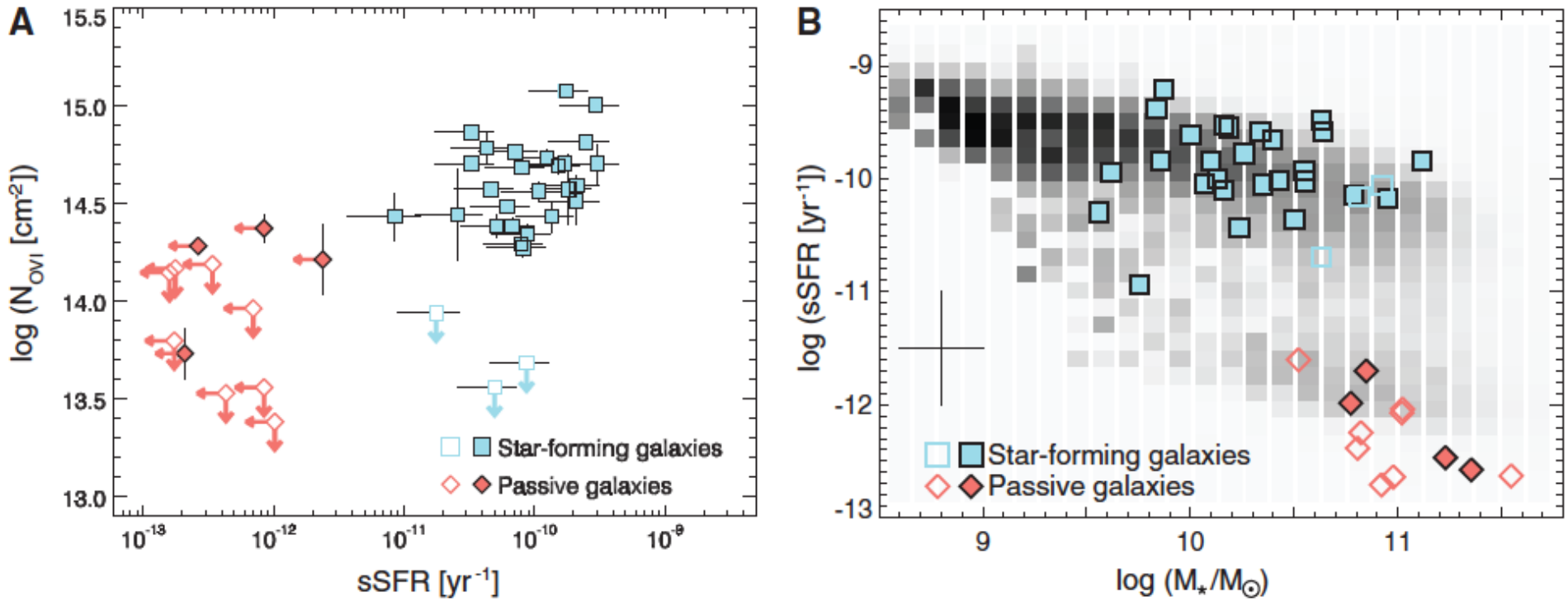
A
15.5
15.0
14.5
14.0
13.5
13.0
log (N_{OVI} [cm^{-2}])
10^{-13}
10^{-12}
10^{-11}
10^{-10}
10^{-9}
sSFR [yr^{-1}]
Star-forming galaxies
Passive galaxies
B
-9
-10
-11
-12
-13
log (sSFR [yr^{-1}])
9
10
11
log ($M_*/M_\odot$)
Star-forming galaxies
Passive galaxies

FIREBALL

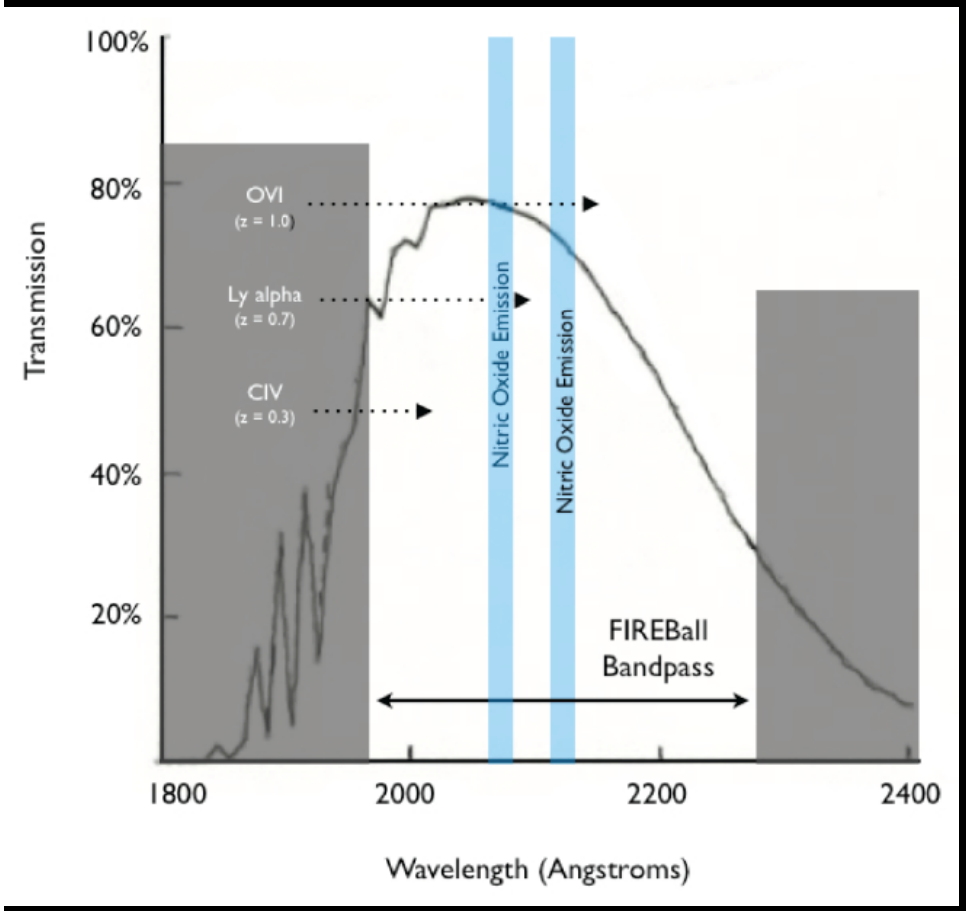
100%
80%
60%
40%
20%
Transmission
OVI
(z = 1.0)
Ly alpha
(z = 0.7)
CIV
(z = 0.3)
Nitric Oxide Emission
Nitric Oxide Emission
FIREBall
Bandpass
1800
2000
2200
2400
Wavelength (Angstroms)